Politecnico di Torino

Politecnico di Torino

MSc in Physics of Complex Systems

A game-theoretic approach to spin models

Candidate: Rebecca Semeria
matr. 301139

Supervisors: Prof. Marco Morandotti
Prof. Luca F. Tocchio

Academic Year 2023/24

Abstract

Monte Carlo algorithms, such as the Metropolis-Hastings one, are commonly used to simulate Ising spin systems. This thesis explores an alternative approach by applying the replicator equation to simulate Ising models, replacing the minimisation of the system's energy with the maximisation of the player's strategy. The analysis focuses on an Ising model for which spins vectors can take orientations corresponding to the principal axes of the system. The replicator equation is modified to take into account interactions between neighbouring spins, both nearest and next-nearest neighbours, as well as external magnetic and nematic fields.

Results show that both the Metropolis-Hastings and the proposed hybrid algorithm reach similar outcomes at a local level. However, although the classical Monte Carlo-based simulations converge to a more globally stable state, the rate of convergence is significantly slower. The hybrid approach, while much faster, presents a more fragmented state, composed of islands of stable states. The introduction of magnetic fields and nematic interactions greatly impacts the system by enhancing stability at the expenses of a slower convergence rate. The analysis suggests that, while the Metropolis-Hastings algorithm remains a robust method for simulating the Ising model, the replicator dynamics with appropriate modifications, provides a faster and effective tool for understanding stability of complex spin systems, by analysing local behaviours.

Contents

Chapter 1

Introduction

Simulating complex physical systems is one of the most challenging and important tasks in computational Physics. These simulations are an important tool in understanding fundamental processes, often revealing critical insight into complex phenomena. The aim of the thesis is to introduce a new approach for simulating extended *Ising systems*, based on the *replicator equation*. Among the theoretical paradigms of Statistical Mechanics, the *Ising model* holds a significant position. Initially developed to describe ferromagnetism, this simple, yet powerful model has been applied across various fields, from Materials Science [1] to Biology [2]. In its simplest form, it provides a flexible framework for modelling pairwise interactions between entities that can take binary states. The model has also been applied in the context of *evolutionary game theory*, to study the evolution of repeated symmetric games [3].

Evolutionary game theory models systems of individuals (like organisms or players) adopting strategies, rules of behaviours that dictate their actions, chosen from a given game-specific set. The state of the system is determined by the frequency of these strategies among individuals at any given moment, changing over time, as individuals die or reproduce. This evolution is governed by the fitness associated with each strategy, which represents the ability of the individual adopting that strategy to survive. The fitness depends on both the considered strategy and the state of the system. In this context, the replicator equation plays a pivotal role, providing a mathematical model for many evolutionary processes. Firstly introduced by Peter Taylor and Leo Jonker [4], it translates the concept of survival of the fittest into a deterministic differential equation. The change of the frequency of each strategy is proportional to the difference between its fitness and the average fitness. Over time, individuals tend to switch to strategies that maximise their fitness and strategies that do better than the average increase in frequency while the less adequate ones decrease.

Despite its significance, the classical replicator equation has limitations. In particular, it fails to account for local interactions between subsets of individuals within the populations, which is fundamental when looking at applications to interacting spins systems. A major development addressing this limitation is the *pair approximation* method, firstly introduced by Matsuda [5]. The method takes into account the importance of local interactions between players by tracking the frequency between neighbouring strategy pairs. In this thesis, we introduce a new approach to this problem, by modifying the equations to include interactions on a

two-dimensional lattice. The aim of this modification is developing a model that can be applied to simulate Ising systems, by considering the maximisation of the individual's fitness instead of the minimisation of the energy.

In this thesis, we study an Ising model, which considers three-dimensional unitary spin vectors allowed to align along the principal axes of a three-dimensional coordinate system. They are placed on a two-dimensional square lattice, where they interact both with nearest-neighbouring and next-to-nearest neighbouring spins. Between nearest-neighbouring points, interactions are extended to include a term penalising orthogonal spins; the effects of magnetic and nematic fields are also considered. The model has been translated into a game theory framework. We assign a probability distribution over the set of strategies to each point of a square lattice, whose evolution follows differential equations with the same structure of the classical replicator. However, when computing the fitness, we shift focus and compute the fitness associated with each individual, accounting for the interactions specified by the structure of the system, rather than the frequency of the fitness. These adjustments provide a local character to the equations, which is reflected in the results of the simulations. Particular attention is given to the addition of external biases in the modified replicator equations, which is not present in the classical model. We propose the addition of a new term in the equation, that shifts the probability in every lattice point towards a given strategy, while being consistent with the model.

The modified equations are then used to construct an algorithm to explore the behaviour of the system. Simulations obtained using the newly proposed replicator-based algorithm are compared to the ones of the *Metropolis-Hastings* algorithm [6], traditionally used to simulate Ising systems. By focusing on these two methods, the goal is to understand how different interactions and external biases affect the behaviour of different spin systems and compare equilibrium configurations and speed of convergence. We must consider that, while the Metropolis-Hastings algorithm depends on the temperature of the system, our new method does not take it into account. Since the system considers deterministic equations, we consider low temperature simulations for the Metropolis-Hastings algorithm at $T = 0.01$.

Firstly, we considered only nearest-neighbouring interactions, with homogeneous coupling constant for both the ferromagnetic and antiferromagnetic case. For both methods, simulations present a similar behaviour at convergence. They both form clusters, that minimise the energy (or maximise the fitness) of interacting lattice points inside them, while receiving a net zero contributions from the ones on the boundaries. The size of these islands is bigger when using the Metropolis-Hastings rule, which is able to reach a more stable state. However, the newly proposed algorithm is much faster, considering the ferromagnetic case it converges in about 400 *sweeps*, in contrast to the 3500 necessary for the Metropolis-Hastings one. The addition of external biases, magnetic or nematic fields, depending on the type of interactions considered, allows the system to reach a more stable configuration. Particularly, for ferromagnetic interactions, when the bias is strong enough, both algorithms converge to the ground state, for which every spin is directed along the same direction. For a more complex system, with competing nearest-neighbours and next-to-nearest neighbour interactions, we observe a much richer convergence behaviour. The ratio of the coupling parameter $r = \frac{J_2}{J_1}$ of interactions between next-nearest and next-to-nearest neighbour spins is important for the state of the system. When its value is small enough, the ferromagnetic interactions between

nearest neighbours dominate and the behaviour of system corresponds to the simple ferromagnetic case, with smaller islands. As it increases, we observe two types of clusters forming: a **striped** and a **vortex-like** configuration. This behaviour is shown in Figure 1.1 for both algorithms, where we considered a model with $r = 5$, which is high enough for these islands to emerge.

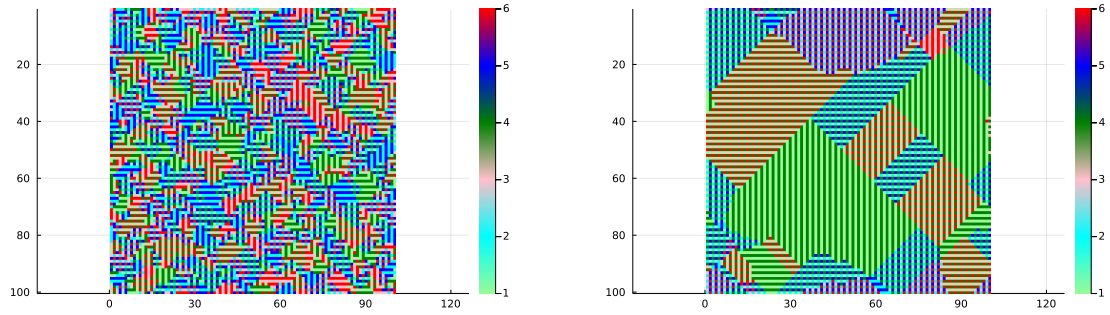

(a) (b)

Figure 1.1: Simulation of an Ising system with ferromagnetic nearest neighbour interactions and antiferromagnetic next nearest neighbour interaction with relative strength given by $r = 5$. The system is simulated using:(a) the replicator-based algorithm (b) the Metropolis-Hastings algorithm

The Metropolis-Hastings algorithm, albeit slower, remains a robust method to analyse the energy landscape and finding a globally stable configuration at convergence. The replicator-based algorithm is faster, but reaches a fragmented locally stable state. This originates from the inherited locality of the method, which limits its ability to achieve global stability. The addition of external biases reduces the advantage in speed of the replicator equation, while allowing it to reach a more stable configuration. Possible future research directions include exploring how incorporating temperature variations may change the behaviour of the replicator-based algorithm, to overcome its locality. Moreover, a mathematical analysis of the model through Γ-convergence could be beneficial to understand its behaviour, in the continuous limit.

The plan of the thesis is the following:

- **Chapter 2** presents a general review of the key concepts of this thesis, their relevance in the thesis and the derivation of the replicator-based algorithm. It introduces the discrete Ising model and its various extensions. Starting from simple nearest neighbour interactions, we progressively introduced more complex interactions, such as magnetic and nematic fields, extended interactions term penalising orthogonal neighbouring spin vectors, and competing next-to-nearest neighbour interactions. The classical tools for the simulation of the Ising model are presented in this section, with a particular focus on the Metropolis-Hasting algorithm. Spatial evolutionary game theory and the replicator equations are briefly presented to serve as a base for the model. Our new algorithm is introduced, by modifying the replicator equation to include both spatial interactions and external biases.

- **Chapter 3** is devoted to the comparison of the newly proposed algorithm and the results that can be obtained with the Monte Carlo methods. For all cases we simulated a 100×100 square lattice. Starting from the known case of the *Prisoner's dilemma* to test the algorithm, we simulate the game, obtaining a state dominated by the second strategy. Then we simulate different systems for both the replicator-based and the Metropolis-Hastings algorithms. We start by considering simple ferromagnetic and antiferromagnetic cases to which we add different external biases, corresponding to a magnetic and a nematic field, respectively. The $J_1 - J_2$ model is considered and analysed for different values the ratio r between the coupling constants, finding transition points as parameter r varies. Also in this case, we consider the addition of a nematic field, which significantly simplifies the behaviour of the system. In all cases, the Metropolis-Hastings algorithm is significantly slower than the new algorithm, but it often reaches a more globally stable state than the replicator equations.

- **Chapter 4** closes the thesis with a summary of the main results, highlighting the performance of the two algorithms and their respective advantages. Moreover, it suggests possible new future developments.

Chapter 2

Methodology

2.1 Ising model

The Ising model was developed by the German physicist *Wilhelm Lenz* in *1920* to describe ferromagnetic properties of materials through interactions between atomic spins. The model was later named after his student *Ernst Ising*, who solved the one-dimensional case, demonstrating the absence of a phase transition. Since then, the Ising model has evolved into one of the most significant and widely studied models in statistical mechanics. Notably, *Lars Onsager* provided an exact solution to the two-dimensional model [7], highlighting its ability to capture essential features of phase transitions, applicable to other types of systems of interacting particles. The model offers a simplified yet powerful representation of interacting systems by representing them as a network of atomic *spins*, binary variables that can take either of two states: up or down. These spins interact with each other, depending on their relative distance, and the model aims to understand how these interactions influence global behaviours, such as magnetization.

To model the interactions between spins, it can be beneficial to define the system on a *graph*. A graph is a mathematical structure representing relationships between objects, determined by two sets V and E. The set V represents the *vertices (or nodes)* of the graph, corresponding to the objects, in this case the spins. The set of *edges (or links)* E represents the relationships between vertices and it corresponds to a subset of all possible connections between vertices, determined by $V \times V$. Therefore, the graph is defined as $G = (V, E)$ and it is called *undirected* , if the edges do not have a specific orientation, or *directed*, when the edges have an orientation; it is called *weighted*, when the edges have specific values assigned to them, representing the strength of the interactions. Specifically, in the context of the Ising model, the spin variables s_i are defined on the sites $i \in V$ taking one of two possible states, $s_i \in \{-1, 1\}$, corresponding respectively to a down or up spin. The main objective of the model is to comprehend how these local interactions influence global properties, such as its overall magnetization. The simplest form of the model considers only interactions between nearest neighbouring spins, but more complex versions can include external magnetic fields, higher order or different types of interactions. The behaviour of the model is driven by its Hamiltonian H, which represents the total energy of the system. The simplest version of the model considers only nearest neighbour interactions and an external magnetic field and the Hamiltonian for such

a system is given by

$$H = -\sum_{(i,j)\in E} J_{i,j} s_i s_j - \sum_{i\in V} h_i s_i. \tag{2.1}$$

In (2.1) the first summation denotes the sum over all pairs of spins s_i and s_j connected by an edge of the graph ($(i,j) \in E$); the coupling parameter $J_{i,j}$ quantifies the strength and the nature of these interactions and can be considered as a weight on the graph. The second summation is taken over each edge of the graph ($i \in V$) and accounts for the influence of an external magnetic field which acts on each spin at site i with a strength h_i. Parameters h_i and $J_{i,j}$ play a crucial role in determining the behaviour of the system. The field establishes a preference for one direction for each lattice site i, proportional to the strength h_i. The coupling parameter $J_{i,j}$ dictates the nature of the magnetic interaction, dividing the system into different classes, depending on its value. When $J_{i,j} \geqslant 0$ for all $(i,j) \in E$, the system is *ferromagnetic*, and the energy contribution given by the interaction term is minimised when spins align with the direction of their neighbours, i.e. $s_i = s_j$ for every pair $(i,j) \in E$. This leads to state with a strong net magnetization, characteristic of ferromagnetic materials, whose intensity is strongly correlated to the temperature of the system. In particular, the *ground state* of the system, which corresponds to the state of lowest energy, is represented by the configuration where all the spins in the system are aligned, i.e. $s_i = s$ for all i points in the lattice. The value of s depends on the sign of the magnetic field: for a homogeneous magnetic field, $h_i = h$ for all $i \in V$, $h > 0$ implies $s = 1$, while $s = -1$ if $h < 0$; for all other cases the configuration may be more complex and other considerations may be taken into account. On the other hand, the system is *antiferromagnetic* when $J_{i,j} \leqslant 0$ for all $(i,j) \in E$; the energy is minimised when adjacent spins are anti-parallel. In this case however, the perfect alternation of opposite spins is not always possible, depending on the structure of the lattice. This can lead to what is known as *frustration*. In frustrated systems, spins cannot simultaneously satisfy interactions preferences from all their neighbours, resulting in multiple and often complex ground state configurations.

In real-world applications, it is common to use a *mixed Ising model*, for which both ferromagnetic and antiferromagnetic interactions coexist, in different regions of the lattice. This occurs when the coupling parameter $J_{i,j}$ takes both positive and negative values for different coupling spins. Such systems reflect real material behaviour, that arises from different situations, such as lattice imperfections given by structural anomalies. In such systems, spins tend to align either parallel or anti-parallel to their adjacent spins, depending on the local variations of the parameters, leading to a wide range of possible configurations and magnetic behaviours.

In even more complex systems, interactions between spins are not limited to nearest neighbouring spins, but may include interactions with next neighbouring spins. These models are known as the $J_1 - J_2$ Ising model, where J_1 represents the nearest-neighbour coupling and J_2 the next-to-nearest-neighbour coupling. In this model, competing interactions between neighbours with different relative distances can lead to frustration, which lead to more complex ground state configurations. For an Ising model, with binary spins, the ground state on a square lattice has been studied, using different methods, including mean field approximation [8], Monte Carlo simulations [9] and Effective Field theory (EFT) [10]. The different studies agree on defining two different phases determined by different ground states, even if the type of transition and values of r are not in agreement. Using an EFT approach,

R. A. dos Anjos et al [10] determined a second order phase transition between a ferromagnetic phase, that emerges for values $r < \frac{1}{2}$, and a super-antiferromagnetic phase, when $r > \frac{1}{2}$. The ferromagnetic phase is determined by the ferromagnetic ground state, while, the super-antiferromagnetic phase is composed by alternated rows of anti-parallel spins.

In this thesis, the Ising model is extended to include six different directions of the spins, and the emerging phases will be more complex, see Section 3.4. Moreover, we focus on different Ising systems, from simple cases with homogeneous ferromagnetic nearest neighbour interactions to more complex systems with competing interactions between neighbouring spins at different relative distances. We will address the problem by performing simulations that are based on the *replicator dynamics*. In particular, as we will see in Section 2.4, the energy minimisation is replaced by fitness maximisation.

The most general model that we will consider is defined on a two-dimensional square lattice with ferromagnetic nearest neighbour interactions, as well as antiferromagnetic next-to-nearest neighbour interactions, both homogeneous in the lattice. A square lattice $N \times N$, with nearest and next-to-nearest neighbour interactions, can be represented by a graph $S = G(V, E)$. The set of vertices $V = \{1, \ldots, N^2\}$ corresponds to the lattice points and the set of edges, defined as $E = E_1 \cup E_2$ contains nearest and next-to-nearest neighbouring pairs of lattice points. In particular, E_1 will contain edges connecting pairs (i, j) such that $|i - j| = 1$, while, the links in E_2 connects pairs (i, j) such that $|i - j| = \sqrt{2}$. The spins are represented as three dimensional vectors restricted to align along the principal axes of the system, in order to provide a simplified yet insightful model for studying the impact of competing interactions. The aim is to conduct a numerical study that functions as a precursor for a future, more rigours analysis, of a limit in a continuous three dimensional vector space. The Hamiltonian of the system includes contributions from an interaction term described by:

$$\begin{aligned} E_{int} &= -J_1 \sum_{(i,j)\in E_1} \vec{s_i} \cdot \vec{s_j} + J_2 \sum_{(i,j)\in E_2} \vec{s_i} \cdot \vec{s_j} \\ &= - \sum_{(i,j)\in E_1} \vec{s_i} \cdot \vec{s_j} + r \sum_{(i,j)\in E_2} \vec{s_i} \cdot \vec{s_j} \,. \end{aligned} \tag{2.2}$$

The summation are taken over $\vec{s_i}$ neighbouring sites in the lattice and the spin at each point in the lattice is represented by a vector that can take values in the set $\big\{(\pm 1, 0, 0,),(0, \pm 1, 0,), (0, 0, \pm 1)\big\}$, which correspond to an alignment with the principal axes of the system. Specifically, the first summation term represents the contributions from interactions between nearest neighbouring spins, at a distance of one lattice spacing $|i - j| = 1$, and it is negative to account for ferromagnetic interactions. The coupling parameter $J_1 > 0$ defines the strength of the interaction and the dot product $\vec{s_i} \cdot \vec{s_j}$ measures the alignment of the spins. The second term accounts for interactions between next-to-nearest neighbour, at a distance of $\sqrt{2}$ lattice spacing; like the first one it depends on the alignment between the spins through a coupling parameter $J_2 \geqslant 0$, and unlike the first one is a positive term to account for antiferromagnetic interactions. The energy contribution is simplified by introducing the relative interaction strength r, defined as the ratio between next-to-nearest-neighbour coupling constants and nearest-neighbour ones: $r = \frac{J_2}{J_1}$. Expressing the energy in terms of r emphasises that the behaviour of the system

depends on the relative strength between J_1 and J_2, rather than their individual values. In Section 3.4 we will explore how the system behaviour changes for different values of r, in the case of competing ferromagnetic next-nearest neighbour and antiferromagnetic next-to-nearest neighbour interactions.

When considering an external magnetic field interacting with the spins, an additional contribution to the energy of the system is introduced. Specifically, if we consider a homogeneous magnetic field $\vec{h} = B\vec{\mu}$, of strength given by the positive parameter B and directed along direction $\vec{\mu}$, the contribution to the energy can be expressed as:

$$E_{mag} = -\sum_{i \in V} \vec{h} \cdot \vec{s_i}. \tag{2.3}$$

This energy contribution considers the effect of the magnetic field and it is minimised when the spins align with its direction $\vec{\mu}$.

Moreover, *nematic* fields are also considered, especially when antiferromagnetic interactions are added to the system. This type of fields introduce anisotropic interactions that maintain a preferred orientation, without restricting the alignment of spins, unlike that in equation (2.3). This characteristic allows spins to be favored both in the parallel and anti-parallel direction of the field. Nematic interactions are commonly found in liquid crystals, for which relative orientations of the molecules are more important than their direction. The contribution to the energy derived from this type of interaction can be expressed by the term

$$E_{nem} = -\sum_{i \in V} |\vec{h}_{nem} \cdot \vec{s_i}|. \tag{2.4}$$

Similar to the classical magnetic field , the homogeneous nematic field can be expressed by $\vec{h}_{nem} = B\vec{\mu}$, where the positive parameter B determines the strength and the vector $\vec{\mu}$ its direction, constituting the preferred orientation axis of the spins. Unlike the classical magnetic field, the term depend on the absolute value of the dot product between $\vec{h}_{nem}$ and the spins $\vec{s}_i$.

We also considered an additional *interaction* term aimed at penalising the contribution from orthogonal nearest neighbouring spins. The term can be expressed as:

$$E_{ext} = -\sum_{(i,j) \in E_1} \nu\big(1 - |\vec{s}_i \cdot \vec{s}_j|\big). \tag{2.5}$$

The summation is taken over all possible pairs $(i, j) \in E_1$ in the system. This additional interaction increases the total energy of the system by a factor $-\nu$ (considering the term $\nu \leqslant 0$) when neighbouring spins are orthogonal to each other, that is $|\vec{s}_i \cdot \vec{s}_j| = 0$, and it does not have any effect when the spins are parallel or anti-parallel to each other. It can also be considered as *asymmetric*, meaning that it penalises the possible orthogonal direction differently. The contribution in this case can be written as:

$$E_{as} = -\sum_{(i,j) \in E_1} \nu^{\vec{\lambda}}_{\vec{s}_i, \vec{s}_j}\big(1 - |\vec{s}_i \cdot \vec{s}_j|\big). \tag{2.6}$$

The energy contribution has the same form as in the symmetric case, except for the strength parameter $\nu^{\vec{\lambda}}_{\vec{s}_i, \vec{s}_j}$ that now depends on the direction of the considered spins. Generally, it can be defined as:

$$\nu^{\vec{\lambda}}_{\vec{s}_i, \vec{s}_j} = \begin{cases} \nu_1 & \text{if } \vec{s}_i = \pm\vec{\lambda} \text{ or } \vec{s}_j = \pm\vec{\lambda}, \\ \nu_2 & \text{otherwise.} \end{cases}$$

Therefore, when at least one of the interacting orthogonal spins is aligned with the direction $\vec{\lambda}$ the penalisation has strength ν_1, while, when neither of them is aligned with $\vec{\lambda}$ it has strength ν_2. Both cases $\nu_1 > \nu_2$ and $\nu_1 < \nu_2$ are analysed.

2.2 Metropolis-Hastings algorithm

After establishing the theoretical framework of the Ising model, understanding how the interactions govern the system, the next step is to study how the model behaves for different sets of couplings. Analytical solutions are often limited to simple cases, making numerical simulations an essential tool for providing insights on the system behaviours, for more complex systems. To simulate the behaviour of the system at finite temperatures, we need to sample from the distribution of possible spin configurations. In statistical physics, the probability of the system of being in a particular configuration S at temperature T is given by the *Maxwell-Boltzmann* factor:

$$P(S) = \frac{e^{-\frac{H(S)}{k_b T}}}{Z}, \tag{2.7}$$

where k_b is the Boltzmann factor, T the temperature of the system, $H(S)$ the Hamiltonian of the configuration and Z the partition function, that sums over all possible configurations. Sampling directly from the distribution can be unfeasible due the computational complexity, especially for large systems, since computing the partition function of the system involves summing over an exponential number of configurations. Monte Carlo algorithms offer an efficient way to sample from the distribution without the need to compute the partition function. One of the most important algorithms is the *Metropolis-Hastings one*, originally developed by *Metropolis et al. [6]* and later generalised by *Hastings* [11]. Its flexibility has made it an essential tool for numerical simulations, for a wide range of applications, from simulating physical systems to estimating posterior distribution for Bayesian analysis. In the context of the Ising model, the Metropolis-Hastings algorithm is used to explore spin configurations in the systems, at non-zero temperatures. Starting from a random configuration of spins, the algorithm constructs a *Markov chain* that, after enough iterations, will eventually converge to the target distribution. The requirement for the method to converge to equilibrium are *ergodicity* and the *detailed balance conditions*, that are both satisfied by the structure of the algorithm.

The set of configuration of the system is explored by proposing at each step random spin flips and accepting it based on the energy difference ΔE between the current and newly proposed state. This process allows transitions between configurations favouring states with lower energy, while still allowing higher energy ones to be explored, proportionally to the temperature T of the system.

In this thesis, the Metropolis-Hastings algorithm is used to simulate the Ising model in each proposed set up, to provide a basis for comparison of the new replicator-based algorithm. The basic steps of the algorithm, modified to take into account the Ising model described in the previous chapter, can be summarised as follows:

1. **Initialisation** of the system: assign a random value to all the spins

2. **Trial moves**: perform $N = L_x \times L_y$ trial moves, or *sweeps* by:

(a) Randomly select one site of the system

(b) Select one between allowed spins

(c) Compute the energy difference $\Delta E = E_f - E_{in}$

(d) A random number g is generated form a uniform distribution over $\left[0, 1\right]$

(e) Accept the change if $\Delta E \leqslant 0$ or $g \leqslant e^{\frac{-\Delta E}{k_b T}}$

3. **Repeat** the process for a given number of sweeps ($N_{sweeps} >> 1$)

To optimize calculations and efficiently compute the change in energy ΔE at each step, we consider the difference in configuration before and after the proposed flip change. Let S be the configuration of the system at time t and S' the newly proposed one at time $t + \Delta t$, when suggesting the flip of spin in position i in the lattice. Since only spin $\vec{s}_i$ changes in the new configuration, all the others remain unchanged, so $\vec{s}_j = \vec{s}'_j$ for all $j \neq i$ given $\vec{s}_j \in S$ and $\vec{s}'_j \in S'$. Consequently, the energy difference depends solely on the localised interactions with spin $\vec{s}_i$, and only contributions from the changed spin can be taken into account, allowing us to restrict calculations only to the neighbouring spin, rather than recalculating the entire energy of the system. Considering all possible energy contributions considered in Section 2.1 the difference ΔE can be expressed as:

$$\begin{aligned}
\Delta E &= E_{fin} - E_{in} \\
&= \sum_{k=1}^{q} J_k \sum_{(i,j)\in E_k} \left(\vec{s_i} \cdot \vec{s_j} - \vec{s_i}' \cdot \vec{s_j}'\right) - \vec{h} \cdot \left(\vec{s_i}' - \vec{s_i}\right) - |\vec{h}_{nem} \cdot \vec{s_i}'| + |\vec{h}_{nem} \cdot \vec{s_i}'| \\
&= \sum_{k=1}^{q} J_k \sum_{(i,j)\in E_k} \left(\vec{s_i} - \vec{s_i}'\right) \cdot \vec{s_j} - \vec{h} \cdot \left(\vec{s_i}' - \vec{s_i}\right) - |\vec{h}_{nem} \cdot \vec{s_i}'| + |\vec{h}_{nem} \cdot \vec{s_i}'|,
\end{aligned} \tag{2.8}$$

where q defines the interaction range. The localised calculation of the energy difference yields a significant reduction of the dimension of each sweep, from being proportional to the dimension of the system to the number of neighbours of the considered spin. This change makes the algorithm particularly well suited for large-scale simulations.

Even though the algorithm is highly effective in simulating spin system, especially investigating temperature-dependent behaviours, it presents limitations when exploring points near phase transitions. As the system approaches this points the algorithm suffers from a critical slow down, leading to lower convergence and longer simulation times. Alternatives have been proposed to address this limitation, each one offering improvements in specific contexts. For example, the *Wolff* algorithm [12] is highly effective in reducing slowing down near phase transition points, since it proposes the flip of entire clusters of spins, but is not particularly useful outside ferromagnetic systems. Another solution is provided by *parallel tempering* [13], which involves simulating the system at different temperatures. By allowing the different simulations to exchange configurations, the exploration of the energy is facilitated avoiding local minima that could trap the system. However, simultaneously carrying out different simulation is computationally expensive. Therefore, although the Metropolis-Hastings is not the only possible method, neither the best in all possible

situations, it provides a robust and flexible framework for simulating spin systems at finite temperature. With the algorithm proposed in this thesis, we provide a novel approach and try to understand how it compares with the Metropolis-Hasting one.

2.3 Evolutionary game theory

The replicator dynamics is an important class of dynamical systems in *evolutionary game theory*. Evolutionary game theory applies the traditional rules of *game theory* to evolving populations, analysing how the population evolves over time and identifying which behaviours persist over time and which eventually go extinct. Each individual in the system adopts a *strategy (or phenotype)*, which affects their behaviour in the system. For example, in a biological context, cells can be considered as players and their strategies are represented by the traits that survival cells pass on to their daughter cells; this can be applied to cancer research [14]. The theory describes a Darwinian process for which the survival of individuals depend on the *fitness* level associated with the adopted strategy, and represents its ability to survive. The fitness is determined by considering both the strategy and the state of the system. At each time step the system is updated: individuals with higher fitness are more likely to reproduce, passing on their strategies to the off-springs, while those with lower fitness die off at higher rate. This process leads to a selection process, similar to biological evolution, where the fittest strategies dominate the population over time.

In classical game theory, individuals in the system often choose one of the available strategies to play as a *pure strategy*; it can be beneficial to generalise this concept and introduce *mixed strategies*. For this types of games, individuals do not choose a definite action, rather they play according to a probability distribution over available actions. For a given set of pure strategies R, a mixed strategy allows a player to select a strategy $\alpha \in R$ with probability σ_α, where $\sigma_\alpha \geqslant 0$ and $\sum_{\alpha \in R} \sigma_\alpha = 1$.

Within the theory, there are two distinct types of games depending on the types of interactions between individuals. For *pairwise contest games* a given individual competes directly against a chosen opponent, randomly selected from the population. This interaction corresponds to a repeated *two-person games* from traditional game theory. In the context of *games against the field* there are no specific opponents to a given individual, but they compete against the entire population. The success of each strategy is determined by the overall state of the system, and the payoff calculates by the strategies adopted by the entire population. An example of games against the field is the *replicator dynamics*, a successful dynamic applied to various problems in different fields, ranging from biology [15] to economics [16], central focus of this thesis.

To explore the replicator dynamics, consider a population of N individuals. Each individual i in the system adopts a strategy α_i from a set of pure strategies $R = \{1, 2, \ldots, n\}$. At any given time t the fraction of the population adopting a given strategy α can be defined as $x_\alpha(t) = \frac{N_\alpha(t)}{N} \in [0, 1]$, given $N_\alpha(t)$ the number of individuals playing α at time t. How the number of individuals playing different strategy changes is important and determines the state of the system, that can be represented as the vector $\vec{X}(t) = \big(x_1(t), \ldots, x_n(t)\big)^T$. The evolution of the state $\vec{X}(t)$ is driven by the relative fitness of each strategy. In particular, strategies that

outperform the population average increase in frequency; conversely, those underperforming decrease. The change in frequency of individuals playing strategy α from time t to time $t+\Delta t$, defined as $x_\alpha(t+\Delta t) - x_\alpha(t)$, is proportional to the difference between the fitness of the strategy and the population average. Since each individual at any time step adopts one of the strategies belonging to the set R, for every time step in the evolution, the states must be constrained to lie on the unit simplex of the n-dimensional Euclidean space, with n the number of strategies of the game: $S_n = \left\{\vec{X}_n(t) : \quad x_\alpha \geqslant 0 \quad \forall \alpha \in R, \quad \sum_{\alpha\in R} x_\alpha = 1\right\}$. The fitness of each strategy f_α is calculated using the *payoff matrix* A, an $n \times n$ matrix whose elements $a_{\alpha,\beta}$ represent the payoff of an individual playing strategy α against one with strategy β. Since each player interacts with every other player in the population, the fitness of any strategy $\alpha \in R$ is determined by taking into account every possible interactions with the other strategies weighted by their frequency. Thus, the fitness of a given strategy α can be calculated as

$$f_\alpha(t) = \sum_{\beta\in R} a_{\alpha,\beta} x_\alpha(t)\,. \tag{2.9}$$

It follows that the average payoff over all possible strategies in R can be defined as

$$\varphi = \sum_{\alpha\in R} f_\alpha(t) x_\alpha(t)\,. \tag{2.10}$$

In a system evolving in discrete time steps, the evolution of the different strategies can be described by the set of equations:

$$x_\alpha(t+\Delta t) = x_\alpha(t) + x_\alpha(t)\big(f_\alpha(t) - \varphi\big), \tag{2.11}$$

for every strategy α in set R . On the other hand, for continuous times, the evolution of the system is governed by the differential equations:

$$\frac{\mathrm{d}x_\alpha(t)}{\mathrm{d}t} = x_\alpha(t)\big(f_\alpha(t) - \varphi\big). \tag{2.12}$$

It is important to note that the simplex S_n is invariant under the equation (2.12), in other words any trajectory starting in S_n remains in S_n. For the discrete equations it holds only for particular values of the matrix A and must be verified. Indeed, for a large enough change, the probability distributions could become negative, while $\sum_{\alpha\in R} x_\alpha = 1$ is still guaranteed by the equations above.

To solve the problem and ensure that the state remains in the simplex S_n, we could consider a time step different than the unitary one. By adjusting Δt to be small enough, the simplex is invariant under the equation. The equation (2.11) can be written as:

$$x_\alpha(t+\Delta t) = x_\alpha(t) + x_\alpha(t)\ \Delta t\ \big(f_\alpha(t) - \varphi\big), \tag{2.13}$$

for every possible α in the set R. The value of Δt does not alter the trajectory of the dynamic, but simply change its velocity by scaling the absolute value of the change Δx_α.

The classical replicator dynamics describes a game against the fields, which assumes that each individual interacts with the population as a whole. In some real-world applications this assumption holds true, for example when modelling interactions of merchants in economics the only important info is the distribution of bids

and asks, for other purposes it can be beneficial to introduce interactions within a smaller group. To expand the theory to incorporate spatial arrangements of the players inside the population, we can introduce *spatial evolutionary game theory*. Individuals are arranged on the vertices of a graph, $S = (V, E)$ where V denotes a finite set of N vertices ($|V| = N$), and $E \subseteq V \times V$ represent the interacting pairs of individuals (i, j). It is assumed that the graph is undirected, so $(i, j) \equiv (j, i)$. Through this lens the classical replicator equations can be thought as the particular case of a game on a fully connected graph. The evolution of the system is still governed by the fitness of the strategies, however, individuals do not interact uniformly with each other in the population, instead they compete solely with the ones connected to them with edges. Therefore, in this case the fitness does not depend only on the considered strategy and the composition of the entire population, but it depends also on the vertex and its connections. This introduces a more realistic dynamic, as individuals are often influenced mostly by the local environment, rather then the entire population. Contrary to the classical model, where the state is determined by the fraction of the population adopting all possible strategies in R, given by $\vec{X}(t)$, in the spatial version, we must take into account the state of each lattice point. In particular, we consider the probability distributions of strategies across vertices of the graph. For each individual, we are interested in understanding how the probability of adopting a specific strategy α, $\sigma_\alpha^i(t)$, changes over time. The spatial localisation of the games means that the fitness of the strategies, and thus their success, varies form player to player, depending on the strategies of their neighbours and the structure of the lattice itself. Taking into account these modifications the fitness of strategy α for a lattice point i can be written as:

$$f_\alpha^i(t) = \sum_{(i,j)\in E} \sum_{\beta=1}^{n} a_{\alpha,\beta}^{i,j}\, \sigma_\beta^j(t). \tag{2.14}$$

The elements $a_{\alpha,\beta}^{i,j}$ of the matrices $A^{i,j}$ represent the payoff associated with the pair interacting vertices i and j, adopting respectively strategies α and β. Each matrix $A^{i,j}$ captures the strategic interactions between each pair of vertices (i, j). The average fitness can be calculated by considering all possible interactions between the connected lattice points i and j, written as:

$$\varphi(t) = \sum_{\alpha\in R} \sigma_\alpha^i(t) f_\alpha^i(t)\,. \tag{2.15}$$

If the considered graph has a weight $\omega_{i,j}$ assigned to each edge $(i, j) \in E$, the formula 2.14 for the fitness can be modified in the following way

$$f_\alpha^i(t) = \sum_{(i,j)\in E} \omega_{i,j} \sum_{\beta=1}^{n} a_{\alpha,\beta}^{i,j}\, \sigma_\beta^j(t). \tag{2.16}$$

This change allows us to shift our focus from examining the system as a whole to concentrating on the individual and their specific interactions. This approach highlights local effects within the system, such as fluctuations or correlations between neighbouring elements, that might be overlooked when considering the system globally.

2.3.1 Application of the Ising model in game theory

The Ising model has been successfully integrated with the replicator dynamics to explore stable states in evolutionary game theory, providing a powerful framework for analysing how the system behaves over time. For symmetric games, where all players are identical, the payoff depends only on the strategy itself, not on the identity of the player. This symmetry simplifies the mapping of the game into the Ising model. Each player can be represented by a point on the lattice, whose structure reflects the interactions between players. In this set up the set of strategy R corresponds to the set of allowed spins and their local interaction determine the total fitness. As the system evolves, it forms patterns analogous to magnetic domains found in ferromagnetic materials, reproducing the same pattern behaviour that can be expected considering the corresponding Ising system [3]. On the other hand, asymmetric games introduce additional complexities. In such games, players are not identical and their fitness depends on the species they belong to, possibly resulting in different payoffs from adopting the same strategy. This asymmetry complicates the adaptation of Ising-like models, as it requires accounting for player-specific payoff differences. Although symmetric games have well established statistical treatments and equilibrium predictions [17], the analysis of asymmetric games through the Ising model is still under development. Recently, *Correira et al.* introduced the Ising model to explain the emergence of correlation in repeated games [18]. The focus of the article is on a game called *Battle of the Sexes* , classic example of an asymmetric game. Battle of the sexes is a two-player game where individuals with conflicting preferences aim to coordinate to reach a favorable outcome. In the article, the game is analysed using game-theoretic tools and a generalised Ising model. Preferences and interactions are described using Ising-like parameters and the players' choice corresponds to an orientation of the spin. The study reveals that the players' strategies become correlated over repeated interactions, eventually stabilising in configurations comparable to the Ising model ground state. *Correira et al.* demonstrate that, even in small networks players, exhibit this correlated behaviour. This model provides an important insight into the network effects in asymmetric games, showing how interactions impact the convergence of the system. This study highlights the intrinsic connection between the Ising theory and the evolutionary game theory, showing how both can be integrated to model complex strategic interactions.

2.4 Replicator dynamics for the Ising model

The model considered in this thesis is defined on a square lattice of size $N \times N$, with $N >> 1$. The lattice can be represented by a graph $S = G(V, E)$, where the set of vertices $V = \{1, \ldots, N^2\}$, corresponds to the lattice points and the set of edges to their connections. To each point of the lattice $i \in V$ is associated a probability distribution over a set of pure strategies R , denoted by σ_α^i, reflecting that we are considering a mixed strategy model. These strategies correspond to the spin vectors in the Ising model. The set of pure strategies is denoted as $R = \{1, \ldots, n = 2h\}$ and it can be divided into two distinct subsets $R_1 = \{1, \ldots, h\}$ which contains the primary strategies and $R_2 = \{(h+1), \ldots, n\}$, which consists of the opposite strategies. For each strategy belonging to R_1 there exists a corresponding opposite

strategy in R_2. This relationship is formalised through the function

$$\text{rev}(\alpha) := \begin{cases} \alpha + h & if\ \alpha \in R_1, \\ \alpha - h & if\ \alpha \in R_2. \end{cases}$$

which determines the opposite strategy α belonging to any of the two subsets. The strategies in the set R_1 can be translated to the principal directions assumed by the spin variables, and their opposite strategies in R_2 correspond to their anti-parallel directions. Specifically, given a strategy $\alpha \in R$, we can associate with α one of the possible orientation assumed by the spin variables $\vec{\alpha}$, and the strategy corresponding to $\text{rev}(\alpha)$ corresponds to the direction $-\vec{\alpha}$. For the Ising model presented in Section 2.1 of this thesis, we define a set of pure strategies R with cardinality $n = 6$, thus $h = 3$. This means that the set of pure strategies is $R = \{1, 2, 3, 4, 5, 6\}$, while $R_1 = \{1, 2, 3\}$ and $R_2 = \{4, 5, 6\}$. The strategies belonging to the set R_1 correspond to the principal directions x, y, z of the three dimensional coordinate system, and thus to the spin vectors $(1, 0, 0)$, $(0, 1, 0)$, $(0, 0, 1)$. On the other hand, the opposite strategies in R_2 represent the opposite directions along each axis, which corresponds to the negative directions in the three dimensional space.

We recall that we focus on the Ising model with nearest and next-to-nearest interactions on the square lattice. Here, the set of edges is defined as $E = E_1 \cup E_2$, containing nearest and next-to-nearest neighbouring pairs of lattice points. In particular, E_1 will contain edges connecting pairs (i, j) such that $|i - j| = 1$, while, the links in E_2 connects pairs (i, j) such that $|i - j| = \sqrt{2}$. A weight $\omega_{i,j}$ can be assigned to each connection, and it depends on its position within the lattice, so that $\omega_{i,j} = p_k$ for every edge $(i, j) \in E_k$, with the same relative distance d_k. In particular, we determine the weights p_k by imposing the following conditions:

- the product $d_k p_k = c$ for each $k = 1, \ldots, q$, where c is constant and equal for every value of k. This ensures that interactions with neighbours at progressively farther relative distances d_k are assigned a progressively larger weight p_k, and their contribution to the fitness of the individual becomes smaller.

- the sum of all the wights of all connections to a given vertex is equal to 1, $\sum_{k=1}^{q} p_k n_k = 1$, where n_k is the number of connections with associated weight p_k, i.e. the number of k^{th} -nearest neighbouring spins. This condition ensures the normalisation of probability distribution.

This construction ensures that nearest neighbour interactions have a greater impact on the total fitness of an individual than next-to-nearest neighbour interactions. The fitness of the strategy α for an individual i is then calculated as:

$$f_\alpha^i(t) = \sum_{k=1}^{q} p_k \sum_{(i,j)\in E_k} \sum_{\beta \in R} a_{\alpha,\beta}^{k;\,i,j}\ \sigma_\beta^j(t). \tag{2.17}$$

In this equation, $a_{\alpha,\beta}^{k;\,i,j}$ is an element of the matrix $A^{k;i,j}$ and corresponds to the payoff obtained by the individual i playing strategy α against its k^{th}-nearest neighbour j playing strategy β , knowing the individuals are at relative distance $|i - j| = d_k$, since $(i, j) \in E_k$. This payoff matrix takes into account contributions to the total fitness from all possible interactions, allowing the possibility of different types

of interactions depending on the relative distance p_k. The average payoff is still described by equation (2.15).

In this framework, the goal is to maximise the fitness of each player i, which is analogous to the minimisation of the energy in the Ising model. As a result, the payoff matrix is constructed based on the contribution to the total energy of the system from the interactions between neighbouring spins. For example, given the strategies $\alpha, \beta \in R$ corresponding to spin vectors in the Ising model aligned along directions $\vec{\alpha}$ and $\vec{\beta}$ respectively , we can construct the payoff matrices $A^{k;i,j}$ by defining their elements through the interaction energy between the k^{th} neighbouring spin i and j

$$a^{k;\,i,j}_{\alpha,\beta} = J_{k;\,i,j}\,\vec{\alpha}\cdot\vec{\beta} \quad \forall \alpha,\beta \in R \quad \text{and} \quad \forall (i,j) \in E \quad \text{and} \quad k = 1,\ldots,q\,, \tag{2.18}$$

where $J_{k;i,j}$ is the coupling parameter for the k^{th}-nearest neighbours i and j . For nearest neighbours, the interactions can be extended to include a penalisation for orthogonal spins, described in equation (2.6). Therefore, the payoff matrix for the nearest neighbour interactions might have an additional term, determined by:

$$a^{1;\,i,j}_{\alpha,\beta} = J_{1;\,i,j}\,\vec{\alpha}\cdot\vec{\beta} + \nu_{\vec{\alpha},\vec{\beta}}\,(1 - |\vec{\alpha}\cdot\vec{\beta}|) \quad \forall \alpha,\beta \in R \quad \text{and} \quad \forall (i,j) \in E. \tag{2.19}$$

In the considered models, the coupling parameters $J_{k;i,j}$ are homogeneous across the lattice, i.e $J_{k;i,j} = J_k$ for every $(i,j) \in E$. This implies that matrices $A^{k;i,j}$ are also homogeneous within the lattices, allowing us to define $A^{k;\,i,j} = A^k$ for every k^{th} neighbour and all pairs $(i,j) \in E$.

The probability distribution associated with each lattice point evolve according to the spatial-discrete replicator equations (described in equation(2.11)), which depends on the difference between the total fitness f^i_α of the considered strategy α for the i individual and its average φ:

$$\begin{aligned}
\sigma^i_\alpha(t+\Delta t) &= \sigma^i_\alpha(t) + \sigma^i_\alpha(t)\Delta\sigma^i_\alpha\Delta t \\
&= \sigma^i_\alpha + \sigma^i_\alpha\,\Delta t\big[f^i_\alpha(t) - \varphi\big] \\
&= \sigma^i_\alpha\left\{1 + \Delta t\sum_{k=1}^{q} p_k \sum\left[\sum_{\beta\in R} a^k_{\alpha,\beta}\,\sigma^j_\beta - \sum_{\gamma\in R}\sum_{\beta\in R}\sigma^i_\beta\,a^k_{\gamma,\beta}\,\sigma^\beta_\beta\right]\right\}.
\end{aligned} \tag{2.20}$$

The time step Δt plays a crucial role in the dynamic impacting its velocity; a larger time scale Δt accelerates the evolution of the system. However, its value must be carefully selected based on the entries of the payoff matrix A, to ensure physically meaningful distribution. Specifically, at each time step the probability distribution must lie on the simplex of the n-dimensional Euclidean space $\mathbb{R}^n$: $S_n = \{\vec{\sigma}^i_\alpha(t) :\ \sigma^i_\alpha \geqslant 0\ \ \forall\alpha \in R\ \ \forall i \in V;\ \sum_{\alpha\in R}\ \sigma^i_\alpha = 1\}$. To maintain this condition, the time step Δt must large enough to allow for fast evolution, but not so large that the probability distribution becomes negative. Therefore, the condition to impose for determining an appropriate time step Δt can be written as :

$$\min_{\sigma^i,\sigma^\beta} \Delta\sigma^\alpha_i \geqslant \frac{1}{\Delta t} \qquad \forall i \in V. \tag{2.21}$$

This ensures that the system evolves within the constraints of the simplex preventing the occurrences of negative probabilities.

2.4.1 External biases

Although the classical replicator equation effectively models many aspects of evolutionary dynamics, it does not take into account external influences that could significantly alter the system trajectory. These external influences could be critical in real-world scenarios, even outside the Ising framework, modelling environmental factors, such as resource availability, that differently impact the survival of strategies, shaping evolutionary outcomes. In Ising systems, external influences are typically represented by magnetic fields, which bias the alignment of the spins towards the field's direction, breaking the symmetry of the system. To incorporate an analogous behavior in the replicator dynamics, we propose the addition of a new term to the classical replicator equation, that represents external biases. In particular, for an external bias of strength defined by the positive parameter B favoring strategy μ the replicator equation becomes:

$$\sigma_\alpha^i(t+\Delta t) = \sigma_\alpha^i \left\{1 + \Delta t\, \Delta\sigma_\alpha^i + \Delta t\, \Delta\sigma_\alpha^{i,B}\right\}. \tag{2.22}$$

Here, $\Delta\sigma_\alpha^i$ is the change in probability of strategy α due to interactions with neighbouring player, as described by the classic replicator dynamics, and $\Delta\sigma_\alpha^{i,B}$ represents the additional change caused by the external bias B. To ensure that the modified equation still align with the principles of the replicator dynamics and preserves the invariance for the simplex S_n, specific conditions must be imposed. These condition ensure that the modified version behaves predictably under the influence of external biases. First, we consider an external bias analogous to a classical magnetic field $\vec{h} = B\vec{\mu}$, with $B \geqslant 0$. Choosing $B < 0$ would simply invert its direction. Indeed the direction $\vec{\mu}$ is preferred when B is positive and undesired when B is negative, resulting respectively in a positive and negative shift of the probabilities. The opposite is true for the direction $-\vec{\mu}$. In this case, the conditions are the following:

1. **Normalisation**: The sum of the changes in probabilities over the set R must be zero to ensure the normalisation condition $\sum_{\alpha\in R}\sigma_\alpha^i = 1$:

$$\sum_{\alpha\in R}\sigma_\alpha^i\left(\Delta\sigma_\alpha^i + \Delta\sigma_\alpha^{i,B}\right) = 0 + \sum_{\alpha\in R}\sigma_\alpha^i\Delta\sigma_\alpha^{i,B} = 0 \quad \forall i \in V, B \geqslant 0. \tag{2.23}$$

2. **Consistency with the original equation**: when no bias is present in the system ($B = 0$), the modified version should reproduce the original form of the equation:

$$\Delta\sigma_\alpha^{i,0} = 0 \quad \forall\alpha \in R \quad and \quad \forall\, i \in V. \tag{2.24}$$

3. **Favoring the biased strategy**; the introduction of the bias should increase the probability of the favored strategy, $\alpha = \mu$:

$$\Delta\sigma_\mu^{i,B} \geqslant 0 \quad \forall\, B \geqslant 0. \tag{2.25}$$

4. **Opposing the opposite strategy**: conversely, the bias should decrease the probability of the strategy corresponding to the anti-parallel direction of the magnetic field, which is $\alpha = \mathrm{rev}(\mu)$:

$$\Delta\sigma_{\mathrm{rev}(\mu)}^{i,B} \leqslant 0 \quad \forall\, B \geqslant 0.$$

5. **Strongest influence**: the bias should exert the strongest positive influence on the favored strategy, $\alpha = \mu$, and the strongest negative on the opposing one, $\alpha = \mathrm{rev}(\alpha)$:

$$\Delta\sigma^{i,B}_{\mathrm{rev}(\mu)} \leqslant \Delta\sigma^{i,B}_{\alpha} \leqslant \Delta\sigma^{i,B}_{\mu} \quad \forall i \neq \mu, \mathrm{rev}(\mu)\ ,\ \forall\, B \geqslant 0. \tag{2.26}$$

The full equation incorporating the proposed adjustment for external biases can be written as:

$$\begin{aligned}\sigma^i_\alpha(t+\Delta t) = \sigma^i_\alpha \Bigg\{ 1 + \Delta t \sum_{k=1}^{q} p_k \sum \Bigg[\sum_{\beta\in R} a^k_{\alpha,\beta}\,\sigma^j_\beta - \sum_{\gamma\in R}\sum_{\beta\in R} \sigma^i_\beta\, a^k_{\gamma,\beta}\,\sigma^\beta_\beta \Bigg] + \\ + \Delta t \Bigg[b(\alpha) - \sum_{\beta\in R} \sigma^j_\beta\, b(\beta) \Bigg] \Bigg\}.\end{aligned} \tag{2.27}$$

The term $b(\alpha)$ represents the external bias of the system that for a classical magnetic field is defined as:

$$b(\alpha) = \begin{cases} B & \text{if } \alpha = \mu, \\ -B & \text{if } \alpha = \mathrm{rev}(\mu), \\ 0 & \text{otherwise.} \end{cases}$$

It can be proven that this formulation does indeed satisfy all of the required conditions, indeed:

1. The sum of the changes introduced by the new term cancels out:

$$\begin{aligned}\sum_{\alpha\in R} \sigma^i_\alpha \Delta\sigma^{i,B}_\alpha &= \sum_{\alpha\in R} \sigma^i_\alpha \left[b(\alpha) - \sum_{\beta\in R} \sigma^\alpha_\beta b(\beta) \right] \\ &= \sum_{\alpha\in R} \sigma^i_\alpha b(\alpha) - 1 \sum_{\beta\in R} \sigma^i_\beta b(\beta) = 0 \quad \forall i, B.\end{aligned} \tag{2.28}$$

   .

2. When the bias $B = 0$, the bias term $b(\alpha)$ becomes zero for every $\alpha \in R$, thus the contribution to the changes due to external influences is zero for every possible strategy.

3. The probability of aligning to the magnetic field is always higher with respect to the case with no magnetic field. Considering $\alpha = \mu$, which implies $b(\alpha) = B \geqslant 0$, the change becomes

$$\begin{aligned}\Delta\sigma^{i,B}_\mu &= b(\mu) - \sum_{\beta\in R} \sigma^i_\beta\, b(\beta) \\ &= B(1 - \sigma^i_\mu + \sigma^i_{\mathrm{rev}(\mu)}) \geqslant \Delta\sigma^{i,0}_\alpha.\end{aligned} \tag{2.29}$$

   since $(\sigma^i_{\mathrm{rev}(\mu)} - \sigma^i_\mu) \in \big[-1, 1\big]$.

   The change $\Delta\sigma^{\alpha,B}_\mu$ is maximised when $\sigma^i_{\mathrm{rev}(\mu)} = 1$ and $\sigma^i_\mu = 0$ which implies $\Delta\sigma^{i,B}_\mu = 2B$, and minimised when $\sigma^i_{\mathrm{rev}(\mu)} = 0$ and $\sigma^i_\mu = 1$, which implies $\Delta\sigma^{i,B}_\mu = B(1 - 1 + 0) = 0$

4. Conversely, considering the strategy opposite to the magnetic field, so $\alpha = \text{rev}(\mu)$ which implies $b(\alpha) = -B \leqslant 0$

$$\Delta\sigma_{\mu}^{i,B} = B(-1 - \sigma_{\mu}^{i} + \sigma_{\text{rev}(\mu)}^{i}) \leqslant \Delta\sigma_{\alpha}^{i,0}. \tag{2.30}$$

since $(\sigma_{\text{rev}(\mu)}^{i} - \sigma_{\mu}^{i}) \in [-1, 1]$. The change is maximised and null when $\sigma_{\text{rev}(\mu)}^{i} = 1$ and $\sigma_{\mu}^{i} = 0$ which implies $\Delta\sigma_{\mu}^{i,B} = B(-1 - 0 + 1) = 0$, and minimised when $\sigma_{\text{rev}(\mu)}^{i} = 0$ and $\sigma_{\mu}^{i} = 1$ which implies $\Delta\sigma_{\mu}^{i,B} = B(-1 - 1 + 0) = -2B$.

5. The change should be maximised for $\alpha = \mu$ and minimised for $\alpha = \text{rev}(\mu)$. Consider:

$$\Delta\sigma_{\text{rev}(\mu)}^{i,B} = B(-1 - \sigma_{\mu}^{\alpha} + \sigma_{\text{rev}(\mu)}^{i}) \leqslant \Delta\sigma_{\mu}^{i,B} = B(1 - \sigma_{m}^{\alpha} + \sigma_{\text{rev}(m)}^{\alpha}).$$

The following also holds:

$$\Delta\sigma_{\text{rev}(\mu)}^{i,B} = B(-1 - \sigma_{\mu}^{i} + \sigma_{\text{rev}(\mu)}^{i}) \leqslant \Delta\sigma_{\alpha}^{i,B} = B(\sigma_{\text{rev}(\mu)}^{i} - \sigma_{\mu}^{i}) \quad \forall \alpha \neq \mu, \text{rev}(\mu). \tag{2.31}$$

The same modified replicator equation can also be applied to more general external biases, favoring different strategies with varying magnitudes, analogous to the effects of a magnetic field applied along different directions. Moreover, in the case of a nematic magnetic field, which favors both a strategy μ and its opposite $\text{rev}(\mu)$ the condition (4) no longer holds, as both directions are favored equally, $\Delta\sigma_{\text{rev}(\mu)}^{i,B} = \Delta\sigma_{\mu}^{i,B}$. For the same reason, the condition (5) becomes $\Delta\sigma_{\alpha}^{i,B} \leqslant \Delta\sigma_{\mu}^{i,B} = \Delta\sigma_{\text{rev}(\mu)}^{i,B}$ for all $i \neq \mu, \text{rev}(\mu)$. In such cases, the bias term is given by:

$$b_{nem}(\alpha) = \begin{cases} B & \text{if } \alpha = \mu, \text{rev}(\mu), \\ 0 & \text{otherwise.} \end{cases}$$

Again, the parameter B is chosen to be positive, as a negative B would simply favor every strategy different than α and $\text{rev}(\alpha)$. Finally, the time step determination remains analogous to the case without magnetic field, with the addition of the new magnetic term. The condition for the distribution to remain valid is given by:

$$\min_{\sigma^i, \sigma^j} \Delta\left[\sigma_{\alpha.int}^{i} + \sigma_{\alpha}^{i,B}\right] \geqslant \frac{1}{\Delta t}. \tag{2.32}$$

2.5 Algorithm

The proposed algorithm follows a similar structure to the Metropolis-Hastings one, featuring a series of updates of the distribution across the lattice. The procedure can be summarised as follows.

1. **Initialisation**: initialise the probability distributions $\sigma_{\alpha}^{i,B}$ randomly for each lattice sites.

2. **Sweeps**: Perform $N \times N$ sweeps:

   (a) Randomly select one site.

(b) Compute the updated probability for each possible strategy α at the selected site i, $\sigma_\alpha^{i,B}(t+\Delta t)$, using the replicator equation (2.27).

(c) Based on the newly computer distribution extract the new played strategy at site i.

3. **Repeat** the process for a given number of sweeps $N_{sweeps} >> 1$.

Initial condition are a key feature of each system, they have a great impact on the converging state. Although initially, *deterministic* ones were considered, i.e. $\sigma_\alpha^i = \delta_{\alpha,s_i}$, given $s_i \sim \text{Uniform}(R)$ for every $i \in V$, they were quickly discarded, since for the replicator equation they define an evolutionary stable state. Consider a point i in the lattice such that its distribution probability is concentrated on strategy s_i $\left(\sigma_\alpha^i = \delta_{\alpha,s_i}\right)$, the lattice points j, such that $|i-j| = d_k$, are considered its k^th-nearest neighbours and they select another s_j strategy $\left(\sigma_\alpha^j = \delta_{\alpha,s_j}\right)$. We consider how any randomly selected strategy α for the lattice point i changes, substituting the selected deterministic initial condition in the replicator equation (2.27), it becomes :

$$\begin{aligned}\sigma_\alpha^{i,B}(t+\Delta t) &= \delta_{\alpha,s_i}\Bigg\{1 + \Delta t \sum_{k=1}^{q} p_k \sum \Bigg[\sum_{\beta\in R} a_{\alpha,\beta}\delta_{\beta,s_j} - \sum_{\gamma\in R}\sum_{\beta\in R}\delta_{\gamma,s_i}a_{\gamma,\beta}\delta_{\beta,s_j}\Bigg] + \\ &\quad + \Delta t\left[b(\alpha) - \sum_{\beta\in R}\delta_{\beta,s_i}b(\beta)\right]\Bigg\} \\ &= \delta_{\alpha,s_i}\Bigg\{1 + \Delta t\sum_{k=1}^{q} p_k \sum\left[a_{\alpha,s_j} - a_{s_i,s_j}\right] \\ &\quad + B\Delta t\left[\delta_{\alpha,\mu} - \delta_{\alpha,\text{rev}(\mu)} - \delta_{\mu,s_i} + \delta_{\text{rev}(\mu),s_i}\right]\Bigg\}.\end{aligned} \tag{2.33}$$

This equation show that values $\alpha \neq s_i$, the updated distribution the updated distribution $\sigma_\alpha^{i,B}(t+\Delta t) = 0$, for any values of $\Delta t, B, \mu, q$ and A, since in this case $\delta_{\alpha,s_i} = 0$. On the other hand, when $\alpha = s_i$ the equation can be simplified as:

$$\begin{aligned}\sigma_{s_i}^{i,B}(t+\Delta t) &= 1 + \Delta t\sum_{k=1}^{q} p_k \sum\left[a_{s_i,s_j} - a_{s_i,s_j}\right] + \\ &\quad + B\,\Delta t\left[\delta_{s_i,\mu} - \delta_{s_i,\text{rev}(\mu)} - \delta_{\mu,s_i} + \delta_{\text{rev}(\mu),s_i}\right] = 1.\end{aligned} \tag{2.34}$$

For every values of $\Delta t, B, \mu, q$ and A. This proves that if $\sigma_\alpha^i(t) = \delta_{\alpha,s_i}$ then $\sigma_\alpha^i(t+\Delta t) = \delta_{\alpha,s_i}$, for every t. Hence, deterministic initial conditions lead to fixed, unchanging states.

Similar considerations could be made for **uniform** initial conditions, i.e.$\sigma_\alpha^i = 1/n$ for every $\alpha \in R$ and every point in the lattice i. Substituting as before the conditions in the lattice in equation (2.27). We obtain

$$\begin{aligned}\sigma_\alpha^{i,B}(t+\Delta t) = \frac{1}{n}\Bigg\{1 &+ \Delta t\sum_{k=1}^{q} p_k \sum\left[\sum_{\beta\in R} a_{\alpha,\beta}\frac{1}{n} - \sum_{\gamma=1}^{n}\sum_{\beta\in R}\frac{1}{n}a_{\gamma,\beta}\frac{1}{n}\right] + \\ &+ \Delta t\left[b(\alpha) - \sum_{\beta\in R}\frac{1}{n}b(\beta)\right]\Bigg\}.\end{aligned} \tag{2.35}$$

To simplify the equation it can be defined the sum over the columns of the matrix A as $sum(\alpha) = \sum_{\beta=1}^{n} a_{\alpha,\beta}$.

$$\begin{aligned}\sigma_{\alpha}^{i,B}(t+\Delta t) = \frac{1}{n}\Bigg\{1 + \Delta t \sum_{k=1}^{q} p_k \sum \frac{1}{n}\left[sum(\alpha) - \frac{1}{n}\sum_{\gamma\in R} sum(\gamma)\right] \\ + \Delta t B\left[\delta_{\alpha,\mu} - \delta_{\alpha,\mathrm{rev}(\mu)} - \frac{1}{n} + \frac{1}{n}\right]\Bigg\}.\end{aligned} \tag{2.36}$$

For most cases considered in this thesis in chapter 3 , matrix A is defined such that the sum over its columns is the same for every row α, so we can define a fixed parameter $sum(\alpha) = sum$ for every $\alpha \in R$, which depends only on the choice of A. Therefore the equation can be simplified as:

$$\begin{aligned}\sigma_{\alpha}^{i,B}(t+\Delta t) &= \frac{1}{n}\Bigg\{1 + \Delta t \sum_{k=1}^{q} p_k \sum \frac{1}{n}\left[sum - \frac{1}{n} n\ sum\right] + \\ &\quad + B\,\Delta t\left[\delta_{\alpha,\mu} - \delta_{\alpha,\mathrm{rev}(\mu)} - \frac{1}{n} + \frac{1}{n}\right]\Bigg\} \\ &= \frac{1}{n}\Bigg\{1 + B\,\Delta t\left[\delta_{\alpha,\mu} - \delta_{\alpha,\mathrm{rev}(\mu)}\right]\Bigg\}.\end{aligned} \tag{2.37}$$

This indicates that in the absence of external biases $\big(B = 0\big)$, the probabilities across all strategies for any point in the lattice remain uniform , $\sigma_{\alpha}^{i,0}(t+\Delta t) = \frac{1}{n}$ if $\sigma_{\alpha}^{i,0}(t) = \frac{1}{n}$, for any time t. However, adding an external bias in the system tilts the probabilities in the direction of the favored strategy μ making uniform initial conditions viable.

As a consequence, randomly distributed probability distributions are chosen as initial conditions.

The Metropolis-Hastings algorithm is strongly affected by the system's temperature, whereas the replicator-based algorithm under consideration does not take temperature into account. In the article [19] *Arne Trauslen et al.* have explored the comparison between the selection parameter $w \in \big[0,1\big]$ to the parameter $\beta = \frac{1}{k_b T}$ in a *Moran process*. The Moran process is a stochastic model that studies the evolution of fixed-size populations. In each iteration, one individual reproduces with a probability proportional to its fitness, replacing a randomly chosen individual, which introduces both selection and randomness into the dynamics. This process continues until one type becomes dominant or one type goes extinct. They proved that in the limit of strong selection processes, for which $w = 1$ and the fitness corresponds to the payoff π, $F = 1 - w + w\pi = \pi$, the Moran process is deterministic corresponding the low temperature case, and thus $T \to 0$ and $\beta \to \infty$. By increasing the temperature, stochastic effects are introduced into the system, which correspond to lowering the value w. For the replicator equations the fitness of corresponds to its payoff, thus $w = 1$. For this reason, we can consider simulations obtained using the proposed algorithm as performed at low temperature an compare them low temperature Metropolis-Hastings simulations.

Chapter 3

Results

3.1 Benchmark

In order to ensure the validity of the proposed algorithm, it was first checked against a known benchmark case. It was considered the case analysed by *V. Pandit et al.* [20], for a game where only two strategies are available to every player, so the cardinality of set R is set to $n = 2$. In the paper the discrete replicator equation is analysed, described in the previous chapter in Section 2.3, (2.11). They focused on the analysis of a system with payoff matrix with structure.

$$A = \begin{bmatrix} 1 & S \\ T & 0 \end{bmatrix}.$$

The choice of the matrix is not restrictive as the dynamic can be proven to be invariant under transformations of the type $A \longmapsto A + \vec{e}\vec{b}^T$, where $\vec{e}$ is a unit vector of n components, n is the number of strategies considered in the dynamic and $\vec{b}$ any vector of n components. The values of the parameters S and T are fundamental for the dynamic. They determine the regions, where the equation satisfies the conditions $x_\alpha(t + \Delta t) \geqslant 0$ and $\sum_{\alpha \in R} x_\alpha(t + \Delta t) = 1$, provided $x_\alpha(t)$ satisfies the same conditions. By adjusting T and S, the type of game being played can be classified based on its equilibrium behaviour. By choosing $T \geqslant 1$ and $S \leqslant 0$, the game belongs to the class of problems known as the *Prisoner's dilemma*. For a simple two player game defined by the same payoff matrix A, defection is a Nash equilibrium point, meaning that once all player chose strategy two, which in this context is known as *defection*, no individual player can improve their outcome by switching strategy, from defecting to *cooperating*. Similarly, in a infinitely repeated Prisoner's Dilemma, defeating is an evolutionary stable strategy [21]. This means that the fraction of players defeating is increasing as the system evolves, while the fraction cooperating decreases. Eventually, the system converges to a state where players consistently choose to defeat, and the fraction of players electing to cooperate goes to zero. Indeed, for equation (2.11), for problems belonging to the Prisoner's dilemma class, the difference $x_2(t + \Delta t) - x_2(t) \geqslant 0$ for every t, and the opposite is true for x_1. The evolution of the system leads to an equilibrium state, for which the first strategy, effectively disappears from the system, while all the individuals choose to adopt the second strategy. For our algorithm, simulations were carried out by considering the replicator dynamics described in the previous chapter in section 2.4, in equation (2.20). So we considered a square $N \times N$ lattice with $N = 100$ with players choosing

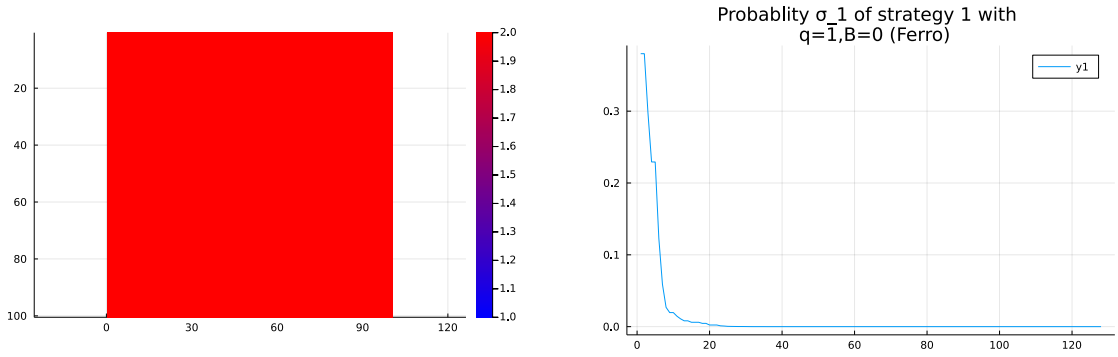

(a) (b)

Figure 3.1: (a) State of the system after 90 *sweeps* showing the dominant stable strategy b) Probability distribution of strategy one for the first point in the lattice, showing the fast extinction of strategy one

strategy from the set $R = \{1, 2\}$ and payoff given by the matrix defined in 3.1, with values of the parameters $S = -0.5$ and $T = 2$, without external influence. Under such conditions we would expect to replicate the equilibrium state discussed above, with the probability of playing the second strategy (defeating) increasing and eventually dominating over the other for every point of the lattice, since the system is homogeneous. To simulate the system, the time step $\Delta t = 1$ was determined by the criterion described by (2.21), ensuring that the system evolves in a stable manner without violating constraints of the probability distributions. The algorithm was run for multiple sweeps, consisting of N^2 trial moves across the entire lattice. After approximately 90 *sweeps*, the systems reaches the ferromagnetic ground state, for which each points adopts the second strategy as dominant. At convergence, as expected, the probability of choosing strategy 1 (denoted as σ_1^k) has dropped to zero, while the probability of choosing the second strategy approaches one, for all the lattice points, $\sigma_2^k \approx 1$ for all $k \in V$. This outcome confirms that the algorithm correctly replicates the predicted behaviour for the Prisoner's dilemma case. Therefore, the algorithm can be tested for more complex and interesting cases. The results are illustrated in Figure 3.1. Panel (a) shows the benchmark configuration after approximately 90 *sweeps*, demonstrating the total dominance of the second strategy. Panel (b) depicts the probability distribution of the strategy one for the first point in the lattice, which shows that, for that particular point the extinction happens around 20 *sweeps*.

The successful simulation of this benchmark case shows the robustness of the algorithm and allows us to explore more complex cases of the game. In the following we will apply the algorithm to study a wide rage of multi-strategy systems, introducing different types of interactions and external biases.

3.2 Ferromagnetic case

In this section, we consider a system for which the payoff matrices are designed to mimic ferromagnetic interactions among nearest neighbouring spins, with homogeneous coupling constant $J = 1$, for every pair $(i, j) \in E$. We consider again a square lattice of size $N = 100$. The payoff matrix can be determined as described in Section

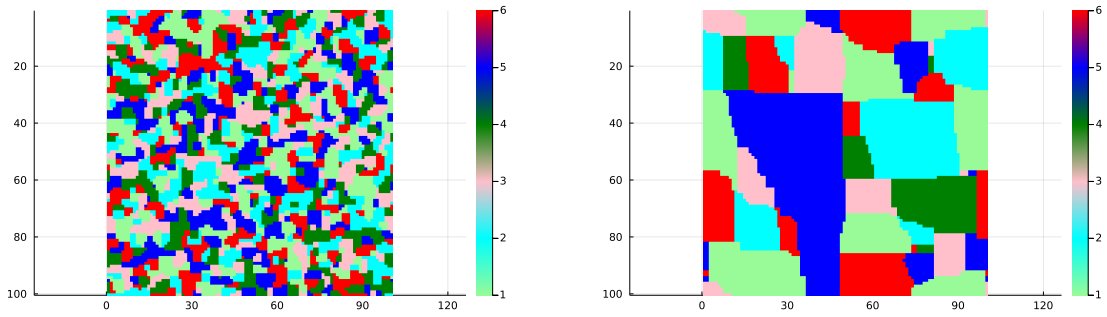

(a) (b)

Figure 3.2: Ground state showing ferromagnetic islands, simulated using (a) the replicator dynamics with ferromagnetic-like payoffs and (b) the Metropolis-Hastings algorithm with ferromagnetic interactions

2.4, by equation (2.19). In this case, the coupling parameter is homogeneous in the lattice, so the payoff depends only on the direction and magnitude of the vectors, not on their position, and the notation can be simplified by considering $a^{i,j}_{\alpha,\beta} = a_{\alpha,\beta}$ for each interaction defined by the pair (i, j). Moreover, no additional interactions were considered, so $\nu^{\lambda}_{\vec{s}_i,\vec{s}_j} = 0$ for every possible vectors $\vec{s}_i, \vec{s}_j$. As a results, when considering ferromagnetic interactions the system favors neighbouring spins with the same strategies, resulting in a configuration with an higher number of interacting pairs with equal strategy. Indeed, the contribution to the fitness of the strategy is given by the diagonal elements of the matrix $a_{\alpha,\alpha} = J\vec{\alpha} \cdot \vec{\alpha} = J$ for every strategy $\alpha \in R$. On the other hand, interactions between opposite strategies are undesirable and penalised in the total payoff, whose contribution is given by the elements $a_{\alpha,\mathrm{rev}(\alpha)} = -J$ for every strategies $\alpha \in R$. All other possible interactions are neutral and have no effect on the fitness of the strategy, providing a zero contribution, since no extended interactions are considered in this case.

Therefore the payoff matrix A_{ferro} when $J_{i,j} = 1$ for every pair (i, j) reduces to the matrix:

$$A_{ferro} = \begin{bmatrix} 1 & 0 & 0 & -1 & 0 & 0 \\ 0 & 1 & 0 & 0 & -1 & 0 \\ 0 & 0 & 1 & 0 & 0 & -1 \\ -1 & 0 & 0 & 1 & 0 & 0 \\ 0 & -1 & 0 & 0 & 1 & 0 \\ 0 & 0 & -1 & 0 & 0 & 1 \end{bmatrix}.$$

The time step was set to $\Delta t = 2$, to ensure that the probability remains positive through the simulations, by requiring the constraint outlined in Equation (2.21). In this case, the expected equilibrium configuration corresponds to a ferromagnetic ground state, for which all players adopts the same strategy. Due to the presence of different strategies contributing zero to the total payoff of each individual, the state could form ferromagnetic clusters which arrange so that neighbouring islands are mostly formed by orthogonal spins. Contributions from the boundary are indeed negligible to the energy of the system and clusters form in the Ising system. In particular, for the replicator equation the probability distributions are expected to converge to a state where $\sigma^k_\alpha = 1$ for every $k \in V$, however the strategy α could

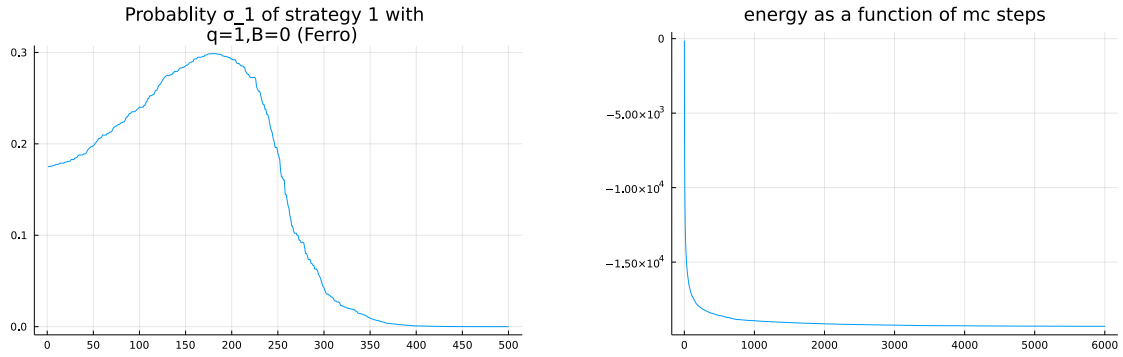

(a) (b)

Figure 3.3: For a ferromagnetic Ising system (a) the probability distribution of strategy one for the first point in the lattice, obtained using the replicator-based algorithm (b) and energy convergence in the Metropolis-Hastings simulations

vary for different points in the lattice. After approximately 300 *sweeps*, $99,27\%$ of points reach this equilibrium point. The dominant strategy is highly dependent on the local initial conditions, and thus the resulting state is composed of ferromagnetic islands, as shown in the Figure 3.2a.

When comparing the simulations using the replicator dynamics to the ones using the Metropolis-Hastings algorithm, it reveals that they both exhibit similar behaviours at convergence, forming ferromagnetic islands. However, the Metropolis-Hastings simulations tend to produce larger clusters. Figure 3.3b shows the results for a system on a $N \times N$ square lattice, with $N = 100$, a small temperature of $T = 0.01$ and homogeneous ferromagnetic interactions $J = 1$ for every nearest neighbouring spin, i, j such that $|i - j| = 1$. The average area of the clusters are calculated and averaged over 200 different simulations and normalised by the size of the system. For the replicator algorithm, the islands have a relative average area of 0.0013 and the Metropolis-Hastings algorithm 0.2, proving that the area of the island is significantly larger in the case of the Metropolis-Hastings algorithm. The perimeter of the islands, normalised by the average area of the islands, is for the replicator and Metropolis-Hastings algorithm respectively $\frac{p_{mean}}{A_{mean}} = 1.3$ and 0.08.

Analysing the two systems using the energy function described in Section 2.1, the replicator simulations will reach convergence faster but to a state with higher energy $E_f = -1.35$, converging quickly but only locally to stable states composed by small ferromagnetic islands. In contrast, the Metropolis-Hastings algorithm, albeit slower, converges to a state with much lower energy $E_f = -1.95$, forming a globally stable configuration. We can observe in Figure 3.3 the velocity of the two algorithms. For the replicator-based algorithm, we look at the evolution of player 1's probability of choosing strategy 1, σ_1^1, shown in Figure 3.3a . The probability quickly stabilises around the value zero ($\sigma_1^1 \approx 0$) after approximately 400 *sweeps*. Figure 3.3b shows the slower evolution of the energy function of the Monte Carlo simulations, which takes up to 3500 *sweeps* to reach convergence.

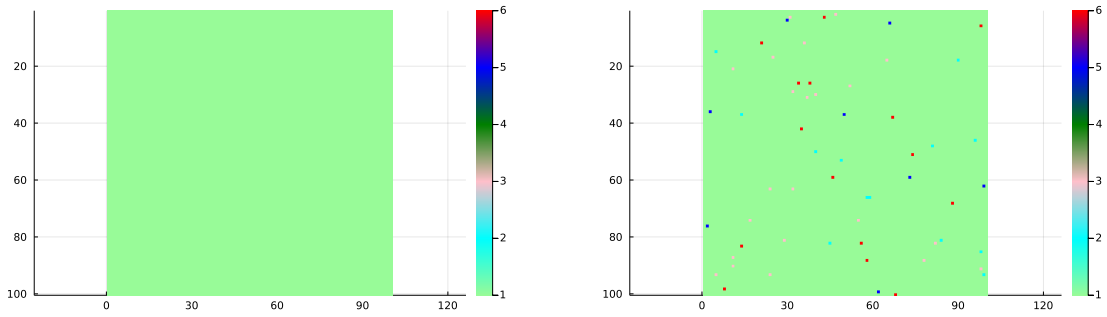

(a) (b)

Figure 3.4: Simulations of a ferromagnetic Ising system with a magnetic field of $B = 0.5$ using the a) replicator-based algorithm (b) and the Metropolis-Hastings algorithm

3.2.1 Adding external biases

To further explore the system dynamics, a bias for strategy one was introduced. In the Ising model is implemented by adding the contribution of a magnetic field directed along the positive direction of the x axis. The replicator equations were modified, as described in Chapter 2, equation (2.27), so that the probability distribution shifts in favor of the corresponding strategy with each step, in this case strategy one. The time step was adjusted for the new structure to ensure stability and it was found to be a function of the strength of the magnetic filed B, $\Delta t = 2 + 2B$.

Considering a magnetic field directed along direction 1, and with strength $B = 0.5$, both simulations were able to reach the ferromagnetic ground state, with normalised energy $E_f = -1.9$. As in the previous case, the replicator-based algorithm was quicker, reaching convergence after approximately *15 sweeps*, while the Metropolis-Hastings algorithm required approximately *50 sweeps*. For both algorithms, the introduction of the external bias is advantageous, as it accelerates convergence and lowers the energy of the system. In this case, the replicator-based algorithm is useful, since it reaches the ground state and it is faster than the Metropolis-Hastings one.

For lower values of B, the system still preserves similar characteristics to the unbiased case, with ferromagnetic clusters slowly increasing in size as parameter B increases. Although both algorithm shows this trend in island size their average area will consistently be larger in ground states reached by the Metropolis-Hastings than in replicator simulations, with the difference decreasing as B increases. In particular, the average perimeter before decreasing reaches a peak at 0.01, as shown in Figure 3.6b for the replicator dynamics, after which it decreases for higher values of B. The system reaches the ground ferromagnetic state and clusters disappear, thus the average perimeter goes to zero for $B \geqslant 0.04$. This behaviour is expected, since as the magnetic field increases, so do the average area and the perimeter of the clusters, as the external bias helps the system to reach a more stable configuration. However, the increase is constrained by the size of the system, and while the area expands until there is only one island with size $N \times N$, as shown in Figure 3.6a, the perimeter starts decreasing when the boundaries between clusters disappear, as the number of islands decreases. Thus, when we apply a bias with strength over

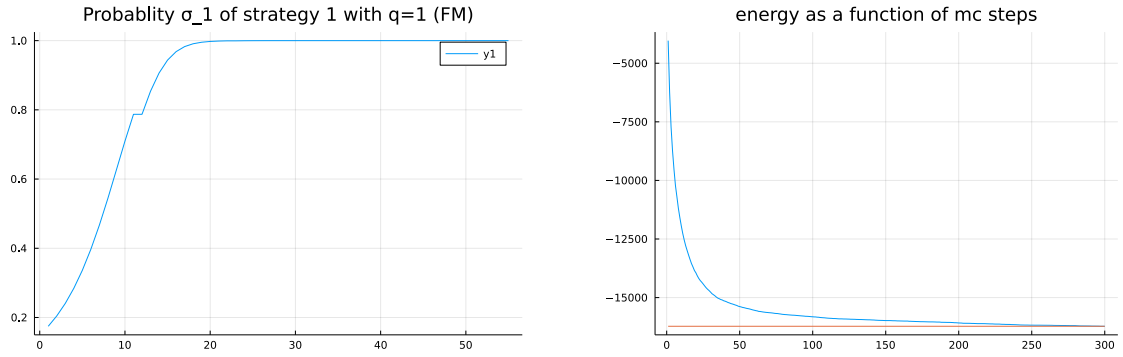

(a) (b)

Figure 3.5: For a ferromagnetic Ising system with a $B = 0.5$ magnetic field (a) the probability distribution of strategy one for the first point in the lattice, obtained using the replicator-based algorithm (b) and energy convergence in Monte Carlo simulations

$B = 0.04$, the islands that form in this configuration have areas comparable to the size of the system. The ratio between average area and average perimeter increases for every value of the magnetic field B.

Adding a nematic field will yield equivalent results to the classical magnetic one, both in behaviours and in numerical results.

3.3 Antiferromagnetic case

In this section, we consider a system designed to mimic an *antiferromagnetic* behaviour, where the coupling constant $J = -1$ for every nearest neighbouring spin pair in the lattice. The payoff matrices $A^{1;i,j}$ are determined as discussed in Section3.2 according to equation (2.18). Specifically, the matrix for antiferromagnetic interactions takes the following form:

$$A_{antiferro} = \begin{bmatrix} -1 & 0 & 0 & 1 & 0 & 0 \\ 0 & -1 & 0 & 0 & 1 & 0 \\ 0 & 0 & -1 & 0 & 0 & 1 \\ 1 & 0 & 0 & -1 & 0 & 0 \\ 0 & 1 & 0 & 0 & -1 & 0 \\ 0 & 0 & 1 & 0 & 0 & -1 \end{bmatrix}.$$

The expected equilibrium configuration for this system corresponds to the antiferromagnetic ground state. This state corresponds of two interpolated square sub-lattices $S_1 = (V_1, E_1)$ and $S_2 = (V_2, S_2)$, such that $V = V_1 \cup V_2$ and $E \subset V_1 \times V_2$, where $S = (V, E)$ represents the original lattice. In this configuration, each point belonging to one sub-lattice adopts the same strategy, while points on the other sub-lattice follow opposite strategies. For instance, if all points $i \in S_1$ select a strategy $s_i = 1$ then every point on the other sub-lattice adopt the opposite strategy, which averages $s_j = 4$ for all $j \in S_2$ for the considered case $n = 6$. This ensures that every two neighbouring points adopt opposite strategies, achieving the antiferromagnetic configuration.

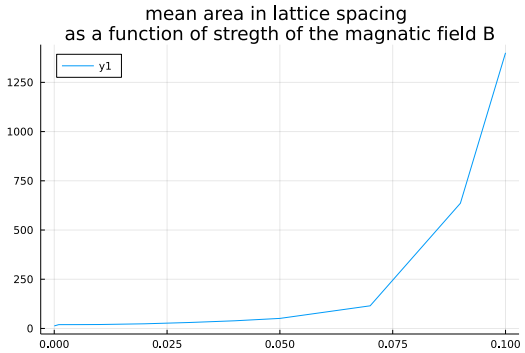

(a)

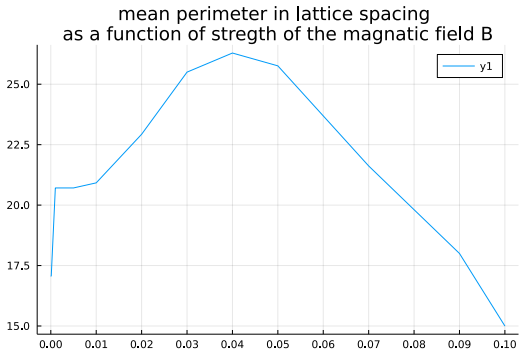

(b)

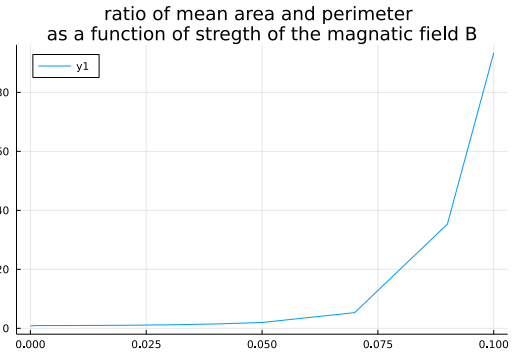

(c)

Figure 3.6: (a) Average area as a function of the strength of the magnetic field B for the replicator-based simulations. (b) average perimeter as a function of the strength of the magnetic field B for the replicator-based simulations. (c) Ratio of average area and average perimeter as a function of the strength of the magnetic field B for the replicator-based simulations.

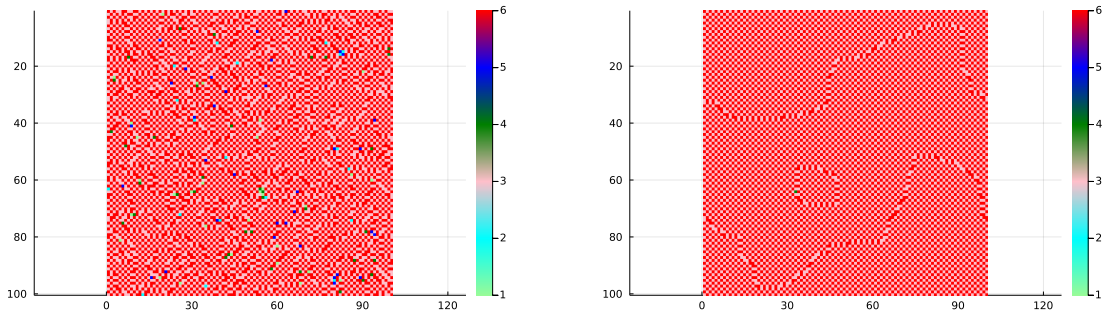

(a) (b)

Figure 3.7: Simulations for an antiferromagnetic system with a nematic magnetic field of $B = 0.2$ using: (a) the replicator-based algorithm and (b) the Metropolis-Hastings algorithm

To simulate the system, we employ once again the equation (2.21) to find the optimal time step, which is the same of the ferromagnetic case $\Delta t = 2$. As shown in figure 3.8a, the system evolves into a configuration of antiferromagnetic islands, composed by the interpolated square lattices S_1 and S_2. The ratio between the average area of these islands and the size of the system is 0.0013 and the ratio between the average perimeter and average area is 1.31. They correspond to the results obtained in the ferromagnetic case. In the replicator simulations, the system converges only locally to the expected behaviour, with a final energy of $E_f = -1.35$. The Metropolis-Hastings simulations yield a similar result, although the configuration presents form larger islands, corresponding to a more stable configurations with smaller energy $E_f = -1.9$, as shown in figure 3.8b.

3.3.1 Adding an external bias

To the system can be added an external bias, however, unlike the ferromagnetic case, a simple magnetic field will not be effective in driving the system global stability. Standard magnetic fields penalise one direction as much as it favours its anti-parallel counterpart, which would be counterproductive. Instead, we can consider a *nematic* magnetic field, along one of the three directions, which proves to be more effective. The bias function $b(\alpha)$ will be defined as:

$$b(\alpha) = \begin{cases} B & \text{if } \alpha = \mu \text{ or } \alpha = \text{rev}(\mu), \\ 0 & \text{otherwise.} \end{cases}$$

In the replicator equation, the nematic bias is applied as described in Section 2.4, and will favour strategy μ and its opposite counterpart $\text{rev}(\mu)$, corresponding to the direction $\vec{\mu}$ and $-\vec{\mu}$ respectively. As with the ferromagnetic case with the magnetic field, the time step is defined by $\Delta t = 2 + 2B$. Simulations show that a bias of strength $B \geqslant 0.2$ is sufficient to drive the system into a predominantly antiferromagnetic ground state, as seen in figure 3.7. The state is dominated by an antiferromagnetic behaviour with some imperfections. These defects are: few remaining spins aligned in a different directions from $\vec{\mu}$ or $-\vec{\mu}$ and more importantly pairs of neighbouring spins parallel to each other. These doublets of parallel spins

do not disappear from the system, even at higher values of B. Indeed, the nematic bias introduces a positive contribution that offsets the negative one, given by the antiferromagnetic interaction between each doublet. On the contrary, the number of neighbours adopting the same strategy slightly increases as B increases.

In conclusion, the addition of a nematic field significantly improves the system's ability to converge towards a stable low-energy configuration, even if doublets are still present.

3.3.2 Penalising interfaces

Another approach at improving the system's stability is introducing an extended interaction that penalises orthogonal neighbouring spins. The desired effect of this interaction would be to reduce the perimeter of the islands. In the context of the Ising model, this additional interaction term was modeled as an added contribution to the total energy described by equation (2.5). In the replicator equation, this penalisation can be incorporated as negative contribution to the total payoff, by adjusting the elements of the matrix A_{pot} as follows:

$$A_{pot} = \begin{bmatrix} -1 & \nu & \nu & 1 & \nu & \nu \\ \nu & -1 & \nu & \nu & 1 & \nu \\ \nu & \nu & -1 & \nu & \nu & 1 \\ 1 & \nu & \nu & -1 & \nu & \nu \\ \nu & 1 & \nu & \nu & -1 & \nu \\ \nu & \nu & 1 & \nu & \nu & -1 \end{bmatrix}.$$

The parameter ν is negative and its value determines the strength of the penalization, transforming the contribution to the total fitness of orthogonal neighbouring spins from zero to negative. This effect discourages neighbouring spins to adopt "orthogonal" strategies, which correspond, given a strategy α, to all strategies $\beta \neq \alpha, \text{rev}(\alpha)$. With an effect analogous to the extended interaction energy contribution, defined in Section 2.1 Equation (2.5).

However, the impact of this extended interaction on the simulations is minimal. In the replicator-based algorithm, while the average perimeter decreases, the ratio average area to average perimeter increases from 1.51 to 2.22, considering values ν from 0 to -2. The Metropolis-Hastings simulations present the opposite effect. For the same values of ν and the ratio decreases instead of increasing, from 2.35 to 1.93. Even when considering larger penalisations, such as $\nu = -10$, the impact on the average perimeter of the clusters remains limited, especially for the replicator-based simulations.

This effect can be better understood by recognising that the replicator-based simulation operate on a local scale. The interactions in this model only modify the behaviour of individual spins, by maximising the fitness calculated only by considering their immediate neighbouring spins. Since these updates do not account for the global structure or larger-scale interactions within the system, introducing a penalization through the interaction matrix also affects only local interactions. As a consequence, the impact of this penalization remains confined to small, isolated regions rather than influencing the overall configuration, and it increases only slightly the size of clusters. Next, we considered the introduction of an asymmetric potential that penalizes orthogonal directions in different ways. The energy contribution

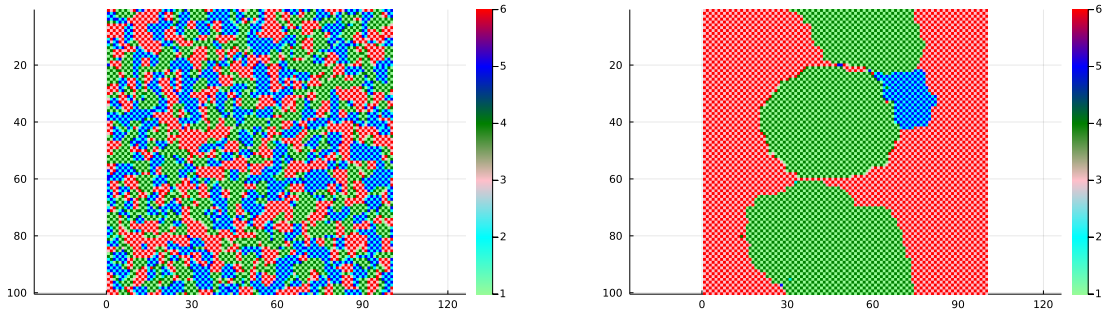

(a) (b)

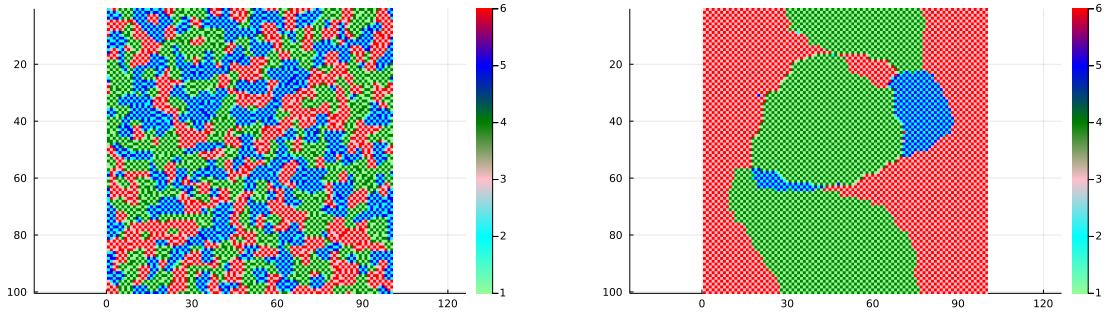

(c) (d)

Figure 3.8: Simulations of an antiferromagnetic Ising model with additional nearest neighbour interactions regulated by the parameter ν, (a) replicator-based algorithm with $\nu = 0$ (b) Metropolis-Hastings with $\nu = 0$ (c) replicator-based algorithm with $\nu = -2$ (d) Metropolis-Hastings with $\nu = -2$

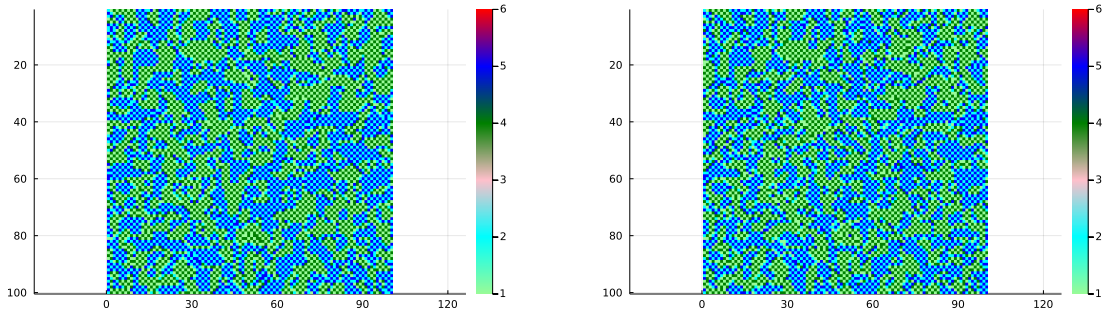

(a) (b)

Figure 3.9: Simulations obtained with a replicator-based algorithm of an antiferromagnetic Ising system with additional nearest neighbour interaction with asymmetric strength defined by ν_1 and ν_2, with values (a) $\nu_1 = 0$ $\nu_2 = -0.5$ (b) $\nu_1 = 0$ $\nu_2 = -0.7$

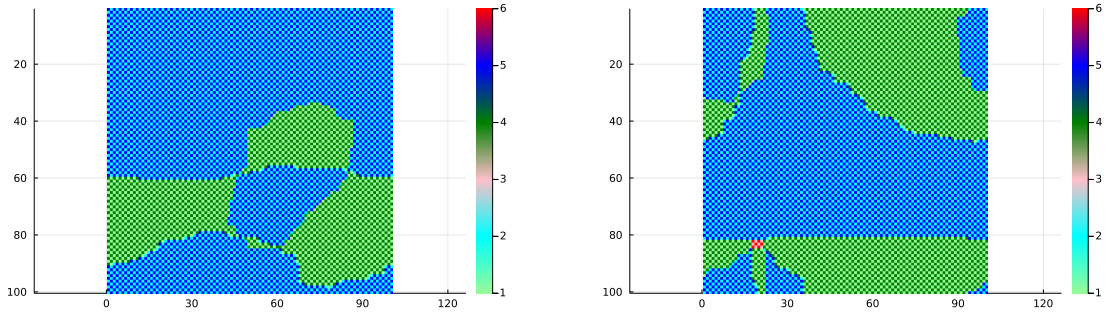

(a) (b)

Figure 3.10: Simulations obtained with the Metropolis-Hastings algorithm of an antiferromagnetic Ising system with additional nearest neighbour interaction with asymmetric strength defined by ν_1 and ν_2, with values (a) $\nu_1 = 0$ $\nu_2 = -0.5$ (b) $\nu_1 = 0$ $\nu_2 = -0.7$

to the Ising system was defined in Section 2.4 as (2.6). In particular, this type of interaction can be used to single out one direction (and its anti-parallel) among the orthogonal ones, by changing the definition of its strength so that $\nu_1 = \nu_3$. The strength parameter can be defined as:

$$\nu_{\vec{s}_i,\vec{s}_j} = \begin{cases} \nu_2 & \text{if } \vec{s}_i = (0,0,\pm 1) \text{ or } \vec{s}_j = (0,0 \pm 1), \\ \nu_1 & \text{otherwise.} \end{cases}$$

As before, in the replicator dynamics, the penalisation is modeled through the payoff matrix. When singling out direction z, which corresponds to the strategy $d = 3$ in the replicator framework, the payoff matrix will take the form:

$$A_{pot} = \begin{bmatrix} -1 & \nu_1 & \nu_2 & 1 & \nu_1 & \nu_2 \\ \nu_1 & -1 & \nu_2 & \nu_1 & 1 & \nu_2 \\ \nu_2 & \nu_2 & -1 & \nu_2 & \nu_2 & 1 \\ 1 & \nu_1 & \nu_2 & -1 & \nu_1 & \nu_2 \\ \nu_1 & 1 & \nu_2 & \nu_1 & -1 & \nu_2 \\ \nu_2 & \nu_2 & 1 & \nu_2 & \nu_2 & -1 \end{bmatrix}.$$

In this case, the effect of the potential is quite large. Consider choosing $\nu_2 > -0.5$, the penalised direction is completely erased from the system, for both simulations. The obtained state has a slightly smaller energy ($E_f = -1.4$) than the simple ferromagnetic case; therefore it is a more stable configuration, even if the convergence speed does suffer from the presence of the potential. Considering the case of a potential that penalises only the orthogonal directions lying on the plane formed by the $d = 1$ and $d = 2$ directions, the parameter are chosen as $\nu_1 < 0$ and $\nu_2 = 0$. The resulting state will be very similar to an antiferromagnetic ground state, with alternated spins in the $d = 3$ and $d = 6$ directions, with some additional imperfections, in the replicator simulations, such as spin doubles, as shown in figure 3.9b In the replicator equation, convergence takes around *350 sweeps* while for the Metropolis-Hastings algorithm, it requires around *5000 sweeps*.

The extended interaction fails to generate significant improvements when all orthogonal directions are penalised uniformly, while it becomes effective when one

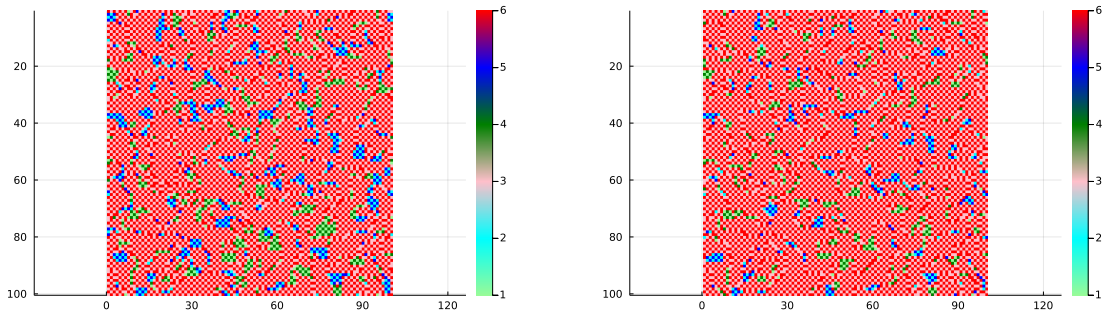

(a) (b)

Figure 3.11: Simulations obtained with a replicator-based algorithm of an antiferromagnetic Ising system with additional nearest neighbour interaction with asymmetric strength defined by ν_1 and ν_2, with values (a) $\nu_1 = -0.5$ $\nu_2 = 0$ (b) $\nu_1 = -0.7$ $\nu_2 = 0$

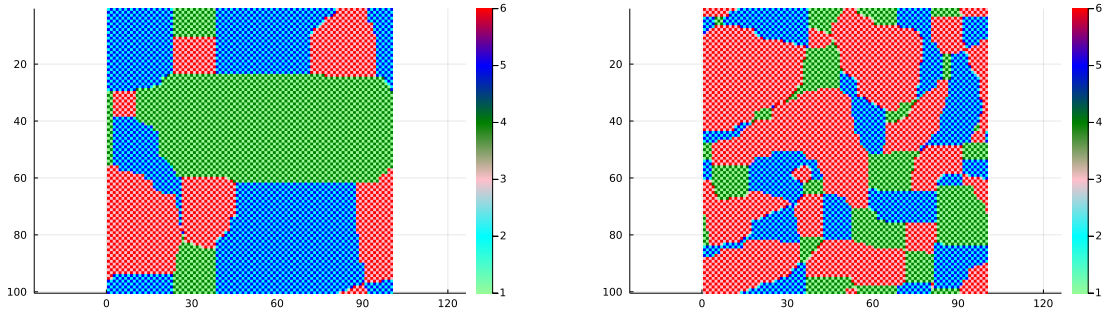

(a) (b)

Figure 3.12: Simulations obtained with the Metropolis-Hastings algorithm of an antiferromagnetic Ising system with additional nearest neighbour interaction with asymmetric strength defined by ν and ν_2, with values (a) $\nu = -0.5$ $\nu_2 = 0$ (b) $\nu = -0.7$ $\nu_2 = 0$

specific direction is singled out for penalisation. In this case, system convergences to a state that resembles the one obtained by considering a nematic field. Since the outcome is similar and the fact that the addition to a nematic field is easier to understand and implement, in the following simulations for a model with competing interactions between nearest and next-nearest neighbour interactions we will focus exclusively on a nematic field.

3.4 $J_1 - J_2$ interactions

In this section, we introduce competitive next-to-nearest interactions to the model, which introduce frustration in the system. The second neighbour interactions are governed by the parameter r, which determines the relative strength of the interactions between the second-nearest neighbours and first-nearest neighbour interactions. We set the first-neighbour interactions to be ferromagnetic, so the matrix of

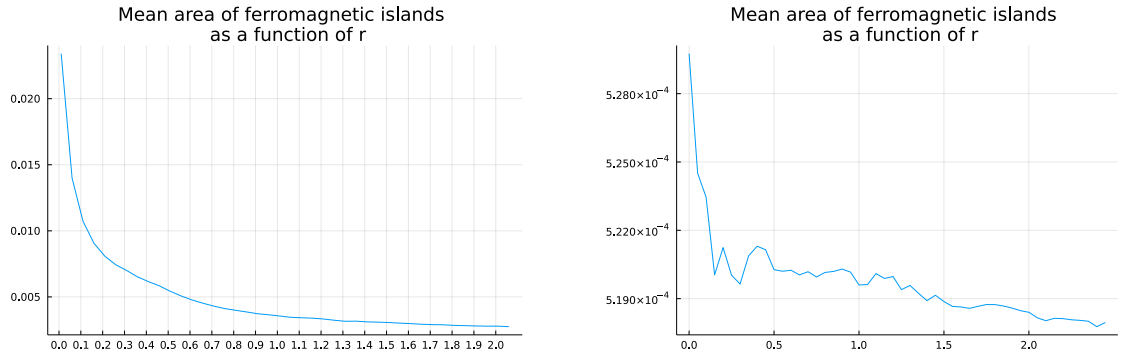

(a) (b)

Figure 3.13: Graph obtained of the normalised average area of ferromagnetic islands as a function of parameter r with (a) the Metropolis-Hastings algorithm (b) and the the replicator-based algorithm

interactions is equal to the one discussed in the ferromagnetic case $A^1 = A_{ferro}$. The second-neighbour interactions are set to antiferromagnetic, represented by the payoff matrix $A^2 = rA_{anti-ferro}$. Since r is a positive parameter and $A_{antiferro} = -A_{ferro}$ the second neighbour interaction can also be expressed as $A^2 = -rA_{ferro}$. The set of equations governing the dynamic of the system takes the form:

$$\begin{aligned}\sigma_\alpha^i(t+\Delta t) = \sigma_\alpha^i \Bigg\{ 1 + p_1\,\Delta t \sum_{i,j:|i-j|=1} \Bigg[\sum_{\beta\in R} a_{\alpha,\beta}\sigma_\beta^j - \sum_{\gamma\in R}\sum_{\beta\in R} \sigma_\beta^i a_{\gamma,\beta}\sigma_\beta^j \Bigg] \\ - r\,p_2\,\Delta t \sum_{k,i:|k-i|=\sqrt{2}} \Bigg[\sum_{\beta\in R} a_{\alpha,\beta}\sigma_\beta^k - \sum_{\gamma\in R}\sum_{\beta\in R} \sigma_\gamma^i a_{\gamma,\beta}\sigma_\beta^k \Bigg] \Bigg\}.\end{aligned} \tag{3.1}$$

In this equation, the first summation accounts for the interactions between the nearest neighbouring points, which are at a relative distance $d_1 = 1$, while the second summation introduces the antiferromagnetic next-to-nearest interactions. The parameter r controls the relative contribution of the second neighbour interactions and as r varies the system exhibits different behaviours, similarly to what was predicted for the Ising model with binary variables [10].

In particular, when r is small, the nearest neighbour interactions dominate and the system behaves similarly to a purely ferromagnetic one, although, with smaller magnetic domains. However, as r increases, the antiferromagnetic next-nearest neighbour interactions become more significant, leading to a much more complex stable state. Particularly, instead of the super-antiferromagnetic phase, described in [10], a more complex state emerges, composed of both alternated rows of anti-parallel spins and by vortex-like structures. The transition from a ferromagnetic to a mixed phase is shown in Figure 3.13, by considering the mean area of the ferromagnetic islands as a function of the parameter r for both methods. Panel (a) shows the behaviour for simulations obtained using the Metropolis-Hastings algorithm. The size of the islands decreases as r increases, at first rapidly for values of $r < 0.2$, then progressively slower. Therefore, in the Metropolis-Hastings simulations, at $r = 0.2$, the system still shows dominance of ferromagnetic interactions and it converges to a state composed of ferromagnetic islands, see Fig.3.15, Panel (a). For $r = 1.0$ antiferromagnetic next-to nearest neighbour interactions are stronger and the system

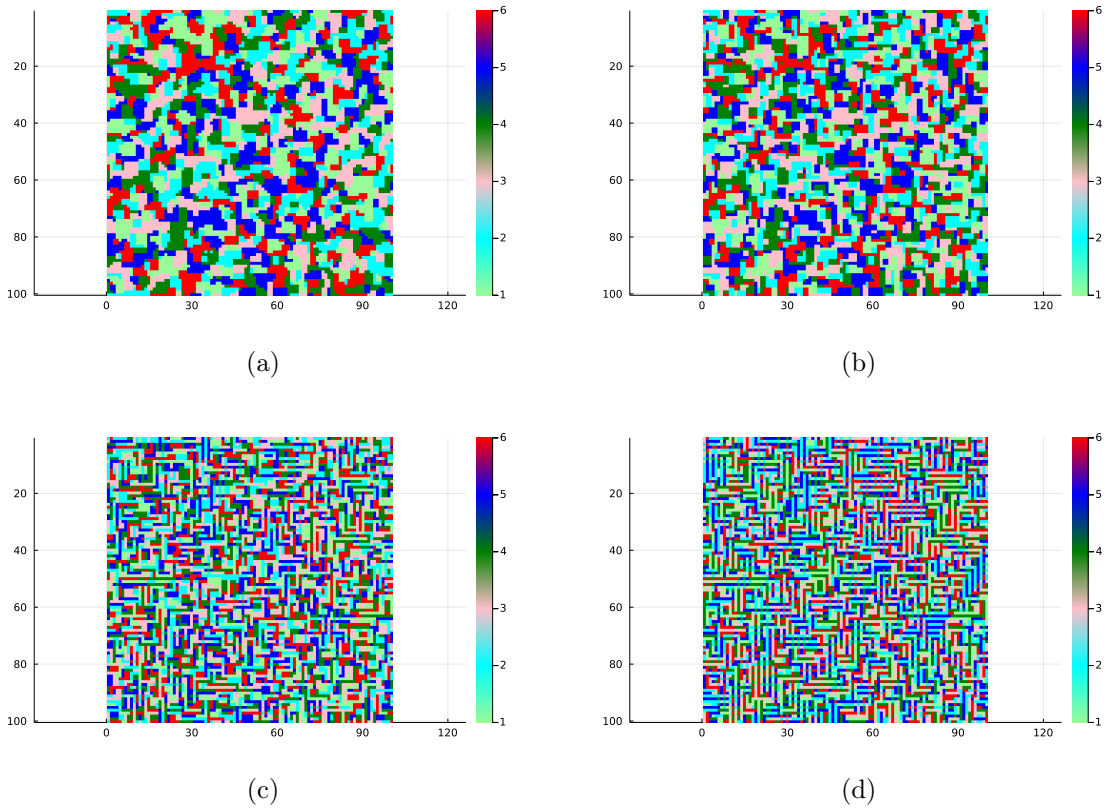

Figure 3.14: Simulations of an Ising system with ferromagnetic nearest neighbour interactions and antiferromagnetic next nearest neighbour interaction with relative strength given by the parameter r. The system is simulated using a replicator-based algorithm for the values of r: (a) $r = 0.02$ (b) $r = 0.05$ (c) $r = 0.08$ (d) $r = 0.1$

has changed phase: the ferromagnetic islands have disappeared and a complex state has emerged, composed of vortex-like patterns and stripes, see Fig.3.15, Panel (d). For the replicator-based algorithm the same transition is present, but it occurs at different values of r. Figure 3.13, Panel (b) shows the behaviour of the size of the ferromagnetic islands as r increases. In this case, the transition occurs at a smaller value of r, and at $r = 0.1$ the system has already started transitioning to a mixed state, see Fig.3.14. Even in this case, the replicator dynamic is faster than the Metropolis-Hastings algorithm, but it convergences to a state with higher energy, considerations that are valid for every value of r.

At a high enough values of r, such as $r = 5$, when antiferromagnetic interactions become important and both simulations stabilise into complex configurations. These convergence states are composed of two distinct types of islands:

- **Type 1**: These islands contain either horizontal or vertical stripes, where spins alternate between parallel and anti-parallel directions.
- **Type 2**: These islands exhibit a vortex-like pattern, where spins alternate between two orthogonal directions and their anti-parallel ones.

In both types of islands, spins adopt opposite strategies to their second nearest neighbour; as a result the energy term corresponding to the next-to-neighbour interactions is minimised. On the contrary, first neighbour interactions provide a net

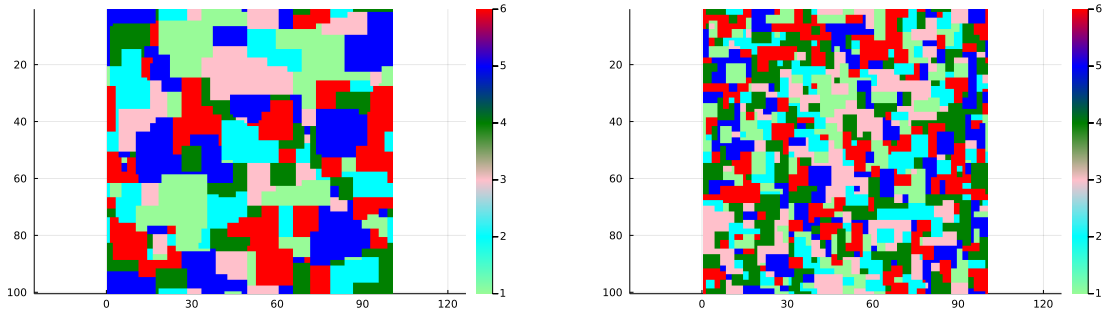

(a)

(b)

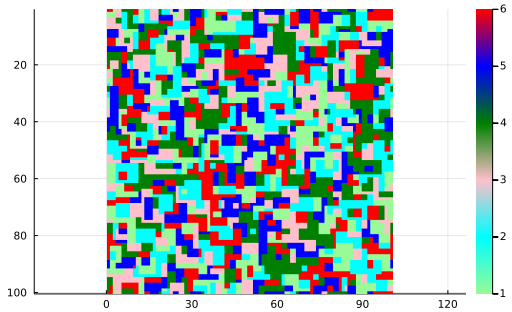

(c)

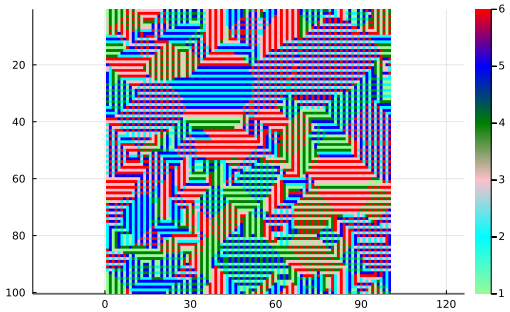

(d)

Figure 3.15: Simulations of an Ising system with ferromagnetic nearest neighbour interactions and antiferromagnetic next-to-nearest neighbour interaction with relative strength given by the parameter r. The system is simulated using the Metropolis-Hastings algorithm, for the values of r: (a) $r = 0.2$ (b) $r = 0.33$ (c) $r = 0.5$ (d) $r = 1$.

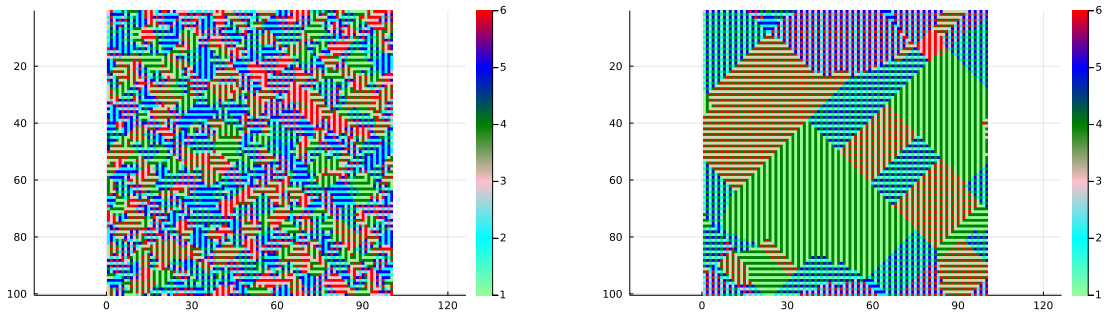

(a) (b)

Figure 3.16: Simulations of an Ising system with ferromagnetic nearest neighbour interactions and antiferromagnetic next nearest neighbour interaction with relative strength given by $r = 5$. The system is simulated using: (a) the replicator-based algorithm (b) the Metropolis-Hastings algorithm.

zero contribution in both cases. For Type 1 islands, half of the nearest neighbours are parallel to the central lattice point and the other half anti-parallel, leading to cancellation. For Type 2 islands nearest neighbours are arranged perpendicularly to the central point, again resulting in a zero net contribution. These patterns are illustrated in Figure 3.16. In particular, Type 1 islands correspond to the super antiferromagnetic behaviour described in Article [10], corresponding to the ground state for an $J_1 - J_2$ Ising model with binary spins. The introduction of four additional directions complicates the behaviour and it introduces vortex-like pattern, Type 2 islands. As discussed above, the Metropolis-Hastings converge to a state with lower normalised energy $E_f = -9.5$, after approximately 3500 *sweeps*, while, the replicator simulation is quicker, only 50 *sweeps* are needed, but it converges to a state with higher normalised energy, $E_f = -7.6$.

3.4.1 Adding an external bias

To further explore the system dynamics, a bias strategy was introduced in the form of a nematic field, which favours a given spin alignment, both parallel and anti-parallel to the magnetic field. Similarly to the antiferromagnetic case, a nematic field directed along direction $d = 3$ was chosen, corresponding to the z direction. When the field strength is sufficiently large, spins that do not align with the field gradually disappear, leaving behind cluster of spins aligned with the preferred directions. In Figure 3.17, we can see the state reached by the replicator-based algorithm for a field of strength $B = 0.1$ for different values of r, around the transition point. As r varies, the influence of the nematic field lead to different changes in the behaviour of the system. For smaller values of r, the state is similar to the ferromagnetic case described in Section 3.2, forming clusters of parallel spins. However, only two directions are present, corresponding to the direction of the nematic field. For $r > 0.2$, the configuration corresponds to the super-antiferromagnetic configuration described in [10], with alternated rows or columns of anti-parallel spins. The introduction of bias effectively erase vortex-like pattern from the system, since directions orthogonal to z are now penalised. Some clusters of parallel spins are still present

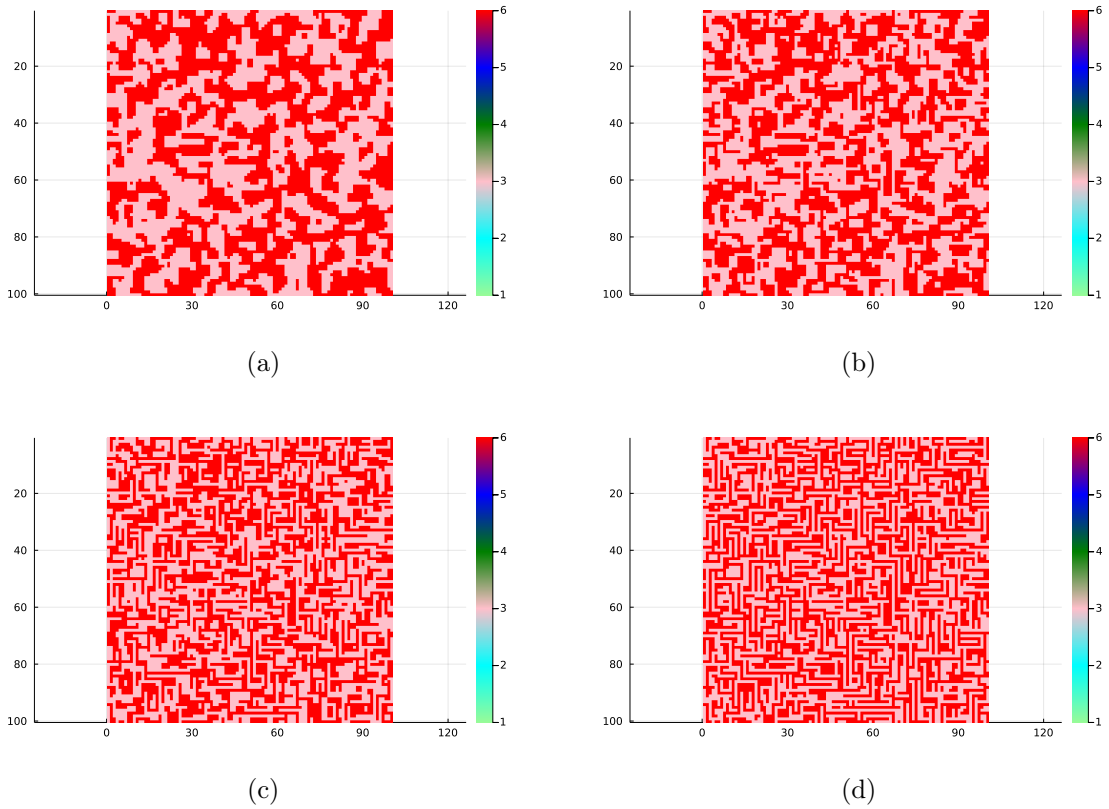

Figure 3.17: Simulations using a replicator-based algorithm of an Ising system with a nematic field of strength $B = 0.1$ and variable ratio between ferromagnetic nearest neighbour interactions and antiferromagnetic next nearest neighbour interactions near the transition point from ferromagnetic dominant to a more balanced model. The ratio r is respectively (a) $r = 0.02$ (b) $r = 0.05$ [c] $r = 0.08$ [d] $r = 0.1$

when $r = 0.1$. For the Metropolis-Hastings algorithm, simulations behavior is the same, but the strength of the field needed to eliminate others direction is larger than for the Metropolis-Hastings. For the same strength of the field, $B = 0.1$, as shown in Figure 3.18, the spins are still able to assume any direction. The only notable difference is in the size of clusters formed by directions $d = 3$ and $d = 6$, which are larger. In this case, it is necessary a strength $B > 0.6$ for the spins to be directed only along z and $-z$. For both algorithms, the introduction of a nematic field simplify the situation, and the configurations obtained are similar to the ones predicted for an Ising model with binary spins in [10]. Indeed, the nematic field effectively reduces the alignment of the spins to the parallel and anti-parallel direction of the introduced field. The system presents the super-antiferromagnetic phase, composed of Type 1 islands, and Type 2 islands disappear from the system.

For the $J_1 - J_2$ Ising model, the comparison between the replicator-based algorithm with nematic field and the ones obtained with Metropolis-Hastings algorithm is also interesting. For $r = 5$, with an added nematic field of $B = 0.1$ the replicator-based algorithm converges to a configuration with normalised energy is $E_f = -7.6$, after 50 sweeps. The Metropolis-Hastings simulations for the same value of r without nematic field, reaches a state with normalised energy $E_f = -1$, after approximately 1000 sweeps. The replicator-based algorithm reaches a state with lower energy, al-

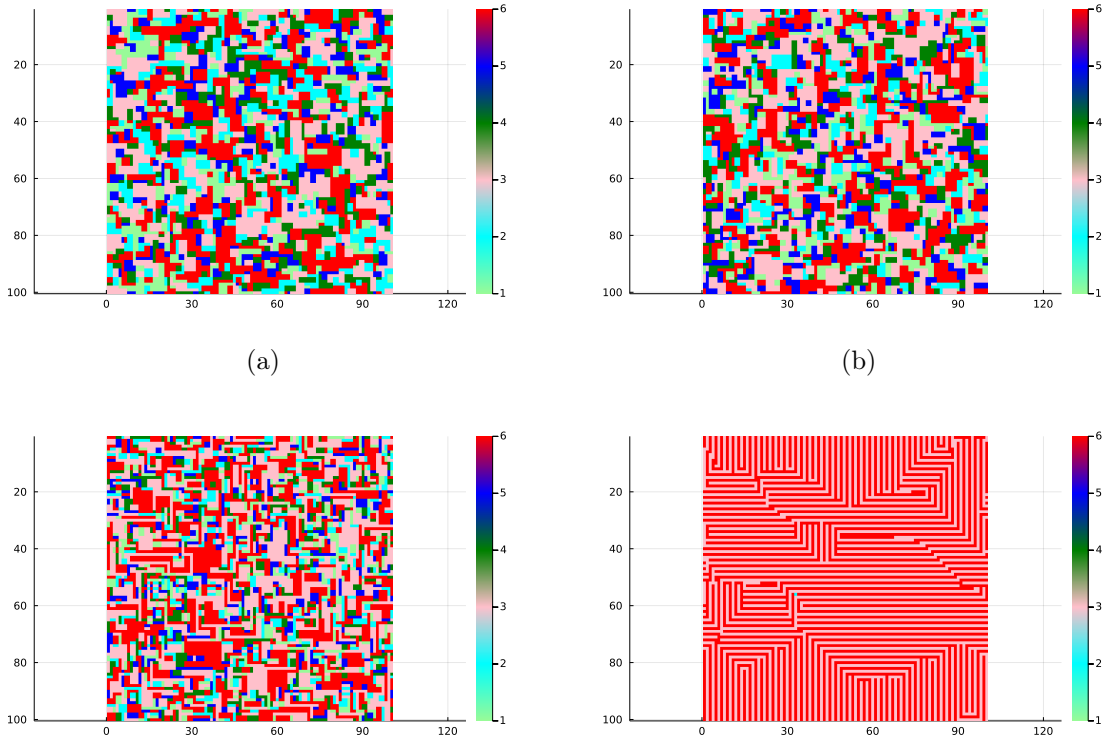

Figure 3.18: Simulations using a Metropolis-Hastings algorithm of an Ising system with a nematic field of strength $B = 0.1$ and variable ratio between ferromagnetic nearest neighbour interactions and antiferromagnetic next nearest neighbour interactions near the transition point from ferromagnetic dominant to a more balanced model. The ratio r is respectively (a) $r = 0.2$ (b) $r = 0.3$ (c) $r = 0.5$ (d) $r = 1$.

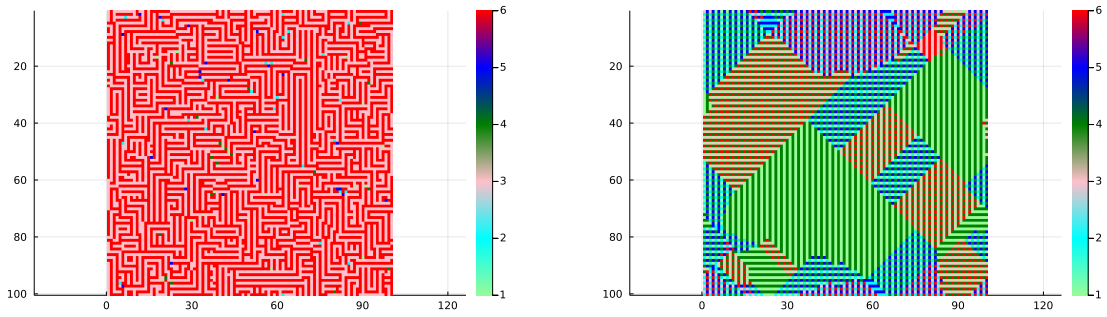

(a) (b)

Figure 3.19: Simulations of an Ising system with ratio between ferromagnetic nearest neighbour interactions and antiferromagnetic next nearest neighbour interactions $r = 5$, respectively obtained using (a) the replicator-based algorithm with an added nematic field of strength $B = 0.1$ (b) the Metropolis-Hastings.

though with different composition, as we can see in Figure 3.19, and it is still much faster than the Metropolis-Hastings. These findings suggests that the replicator dynamics could be a valid alternative to simulate Ising systems, and external biases could be an useful tool to help the system reach a more stable configuration faster.

Chapter 4

Conclusions

In this thesis, we have proposed a novel approach to simulating Ising models, based on the replicator equation. In this new method, energy minimisation is replaced with fitness maximisation in order to drive the system toward a stable configuration. The proposed algorithm delves into the simulations of different extended Ising systems with six different directions of the spin variable, and it is compared to the results obtained with the well-known Metropolis-Hastings algorithm. Our aim is to understand the comparative performance of these algorithms in terms of convergence speed and stability of the resulting spin configurations.

The algorithms were tested against a series of case studies, ranging from simple nearest-neighbour interactions (both of ferromagnetic and antiferromagnetic type) to a more complex model with competing nearest neighbour and next-to-nearest neighbour interactions. The obtained results show that the Metropolis-Hastings algorithm excels at finding globally stable states, by minimising the system's energy more efficiently. This global stability arises from an effective exploration of the energy landscape. On the other hand, the replicator-based algorithm converges faster, even though to a more fragmented locally stable state. These states are characterized by the formation of clusters of spins that replicate locally the behaviour of the more stable states found by the Metropolis-Hastings algorithm, suggesting that the new method prioritise faster solutions, only locally stable. This feature makes the new approach suitable to be used when the size of the system is extremely large, or in much more complex cases, where convergence using the Metropolis-Hastings algorithm requires a long computational time.

Magnetic or nematic fields are also considered in the dynamics. The addition is straightforward in the Metropolis-Hastings algorithm, for which only the energy calculation must be adapted, while for the replicator-based method, a new approach is proposed to include the effects of external biases, maintaining the principal features of the replicator equation. When external magnetic fields are introduced, both algorithms display a predictable shift in spin alignment towards the favored direction. Both algorithms are able to reach a more stable state and for high enough strength of the bias their convergence state corresponds to the ground state of the model. Moreover, the convergence speed slightly decreases, with respect to the unbiased case. Considering a system with nearest-neighbour ferromagnetic interactions, simulations with the replicator-based algorithm converge after approximately 400 *sweeps*, while it decreases to around 20 *sweeps* when adding a bias of strength $B = 0.2$. The same effect is present in the Metropolis-Hastings simulations, from 3500 to 50 *sweeps*,

for the same cases, but, even though the improvement is greater in the Metropolis-Hastings case, the replicator-based algorithm reaches the same convergence state faster. When considering an Ising model with competing interactions among neighbours at different relative distances, we observe a richer convergence state. The behaviour of the system is highly dependent on the ratio $r = J_2/J_1$ between the coupling constants. When r is small enough, ferromagnetic nearest-neighbour interactions dominate and the system is comparable to one with ferromagnetic interactions alone, with slightly smaller islands. As r increases, a more interesting mixed state emerges, composed of two types of clusters: one where alternated anti-parallel spins are arranged in stripes and the other composed of orthogonal spins in a vortex-like configuration. This transition occurs at different values of r for the two algorithms, for Metropolis-Hastings simulations the parameter must be at least $r = 1$ to observe this behaviour, while for the replicator-based algorithm it is enough to chose $r > 0.1$ for these new clusters to emerge. Finally, adding an external nematic field reduces the complexity of the patterns of the stable states, by shifting the spins towards the direction of the bias. This addition does not change the transition from a ferromagnetic to mixed-state, that occurs around the same values of r, but the resulting configuration is less complex. The vortex-like islands are erased from the system, leaving only striped ones, with spins directed parallel and anti-parallel to the field, which corresponds to the super-antiferromagnetic ground state analysed in [10].

In conclusion, this thesis has demonstrated the applicability of the replicator equation as a viable alternative to the Monte Carlo-based Metropolis-Hastings algorithm for simulating Ising spin systems. Through a series of case studies, the proposed algorithm was shown to converge more rapidly to locally stable states, at the cost of settling with more fragmented configurations. This approach can therefore be considered in scenarios where local interactions are crucial, global stability is less relevant, and faster simulations are required, whereas the Metropolis-Hastings algorithm remains the preferred choice for systems that demand global stability.

4.1 Future developments

This works aims to be a computational foundation for future, more rigorous developments. One potential exploration could be incorporating the temperature dynamics to study phase transitions more in depth. The Metropolis-Hastings algorithm is heavily influenced by the temperature of the system. On the other hand, the considered replicator-based algorithm does not incorporate these effects. Following the comparison made in [19], we considered the replicator-based simulations as low-temperature ones. A development in this direction could be considering a similar comparison and modifying the replicator algorithm to include temperature effects. This addition would introduce stochastic effects in the model and could help the system to overcome local effects.

Our study is also structured as a basis for a future, more rigorous analysis of the continuous limit; this is typically dealt with in the framework of Γ-convergence [22, 23]. Analytical studies of similar systems were carried out for $J_1 - J_2$ and $J_1 - J_2 - J_3$ models in [24] and [25], respectively.

A one-dimensional spin chain with competing interactions between nearest and next-nearest neighbouring spins is considered in [24], where the study focuses on

a frustrated ferromagnetic and antiferromagnetic spin chain with vanishing spacing on the one-dimensional torus for low-dimensional magnets at zero temperature. Using a variational approach, the authors aim to understand the ferromagnetic-to-helimagnetic transition point, at values of the ratio $r = J_2/J_1$ approaching the transition point from below. The results show the emergence of a chiral ground state. The scale of the chirality depends on the scaling distance between the position of the spins in the chain and the distance from the transition point.

The problem in a two-dimensional square lattice with the introduction of third-nearest-neighbour interactions is studied in [25], where a frustrated $J_1 - J_2 - J_3$ spin model is considered on a square lattice, again focusing on the ferromagnetic-to-helimagnetic transition, as the lattice spacing vanishes. The study explores how the competition between the three interactions leads to complex magnetic patterns, such as helices of different chiralities. The analysis shows that the system presents two regions, characterized by different ground states. When $r_1 = J_1/J_3 < 2$, the system has a helical ground state, where spins form helices whose chirality depends on the values of r_1 and $r_2 = J_2/J_3$. As r_1 increases, the system tends to a ferromagnetic ground state, where all spins are aligned.

Together, these studies show how competing interactions drive the emergence of chiral states and phase transitions in Ising systems, highlighting that the ground state of the system changes as the relative strength of the competing coupling constant varies. In particular, when J_2 and J_3 are strong enough, respectively for the first and second considered case, the ground state is complex and presents helices. This behaviour is similar to the vortex-like structure observed in our numerical solutions, suggesting that a rigorous analysis could reveal similar results.

In view of this similarity, while our algorithm based on the replicator equations has some limitations, we are confident that it may offer a compelling alternative for specific problems, especially when looking at the local stability of spin system.

Appendix A

Julia Code

Simulations were carried out using the following Julia function, that describes the replicator-based algorithm described in this thesis. Given an $N \times N$ square lattice with n the number of strategies that can be adopted by each point, in the following $sigma$ is a N^2-vector of vectors with n components that represents the probabilities associated with each point in the lattice at the time t considered, q the farther interacting neighbours present in the model, $neig$ is a N^2-vector of vectors whose k^{th} component contains all k^{th}-nearest neighbours, the vector of matrices a specify the matrix of interactions for each k^{th}-nearest neighbours, b a n-vector defining the external bias $\vec{h} = B\vec{\mu}$, and, finally, $Delta\_t$ the time step of the system.

```
function replicator_step(sigma, N, n, q, neig, p, a,b,
 ↪  Delta_t)
    #(a) randomly select one of the N^2 lattice  sites
        i= rand(1:N^2)
        nei=neig[i,:]

    #(b) compute the updated probabilities for the
     ↪  individual i, by calculating the change Delta_u(m)
     ↪  for each startegy m, using the modified-replicator
     ↪  equation.
        Delta_u=zeros(n) #initialise to zero the change in
         ↪  probabilities

        for k in 1:q
            for n in nei[k]
                Delta_u+=(a[k]*sigma[n]).-sigma[i]'*
                 ↪  a[k]*sigma[n]#Delta_u+=(a[k]*sigma[n]).-sigma[i]'*
                 ↪  a[k]*sigma[n] #change due to the
                 ↪  interactions
            end
            Delta_u=Delta_u.*p[k]
        end
        Delta_u+=b.-sigma[i]'*b #contrinution from an
         ↪  external bias of weight b

        #update the probabilities
```

```
18          sigma[i]+=sigma[i].*Delta_u./R
19
20          #control for normalized weights to avoid
             ↪  computational errors: if the sum of the
             ↪  probabilities associated with point l are not
             ↪  normalised we normalise them.
21              my_sum=sum(sigma[i])
22              if !isapprox(my_sum, 1, rtol=1e-9)
23                  sigma[i]=sigma[i]./my_sum
24              end
25      return sigma
26  end
```

Bibliography

[1] I. Y, T. Anazawa, F. Kumasaka, and H. Jippo, "Optimization of the composition in a composite material for microelectronics application using the Ising model," *Scientific Reports*, vol. 11, Feb 2021.

[2] K. Simpson, A. L. J. Keymer, and F. Federici, "Spatial biology of Ising-like synthetic genetic networks," *BMC Biology*, vol. 21, Sep 2023.

[3] M. Kikkawa, "Statistical mechanics of games: Evolutionary game theory," *Progress of Theoretical Physics Supplement*, vol. 179, pp. 216–226, 03 2009.

[4] P. D. Taylor and L. B. Jonker, "Evolutionarily stable strategies and game dynamics," *Bellman Prize in Mathematical Biosciences*, vol. 40, no. 1, pp. 145–156, 1978.

[5] H. Matsuda, N. Ogita, A. Sasaki, and K.Sato, "Statistical mechanics of population: The lattice lotka-volterra model," *Progress of Theoretical Physics*, vol. 88, pp. 1035–1049, 1992.

[6] N. Metropolis, A. W. Rosenbluth, M. Rosenbluth, A. H. Teller, and E. Teller, "Equation of state calculations by fast computing machines," *The Journal of Chemical Physics*, vol. 21, pp. 1087–1092, 06 1953.

[7] L. Onsager, "Crystal statistics. i. a two-dimensional model with an order-disorder transition," *Phys. Rev.*, vol. 65, pp. 117–149, Feb 1944.

[8] S. Katsura and S. Fujimori, "Magnetization process and the critical field of the ising model with first- and second-neighbour interactions," *Journal of Physics C: Solid State Physics*, vol. 7, p. 2506, jul 1974.

[9] E. López-Sandoval, J. Morán-López, and F. Aguilera-Granja, "Cluster variation method and monte carlo simulations in ising square antiferromagnets," *Solid State Communications*, vol. 112, no. 8, pp. 437–441, 1999.

[10] R. A. dos Anjos, J. R. Viana, and J. R. de Sousa, "Phase diagram of the ising antiferromagnet with nearest-neighbor and next-nearest-neighbor interactions on a square lattice," *Physics Letters A*, vol. 372, no. 8, pp. 1180–1184, 2008.

[11] W. K. Hastings, "Monte carlo sampling methods using markov chains and their applications," *Biometrika*, vol. 57, pp. 97–109, 04 1970.

[12] U. Wolff, "Collective monte carlo updating for spin systems," *Phys. Rev. Lett.*, vol. 62, pp. 361–364, Jan 1989.

[13] R. Swendsen and J. Wang, "Replica monte carlo simulation of spin-glasses," *Physical Review letters*, vol. 57, Dec 1986.

[14] B. Wölfl, H. te Rietmole, M. Salvioli, A. Kaznatcheev, F. Thuijsman, J. S. Brown, B. Burgering, and K. Staňková, "The contribution of evolutionary game theory to understanding and treating cancer," *Dynamic Games and Applications*, vol. 12, June 2021.

[15] M. Paczkó, E. Szathmáry, and A. Szilágyi, "Stochastic parabolic growth promotes coexistence and a relaxed error threshold in rna-like replicator populations," *eLife*, vol. 13, p. RP93208, apr 2024.

[16] A. Z. Dragicevic, "The price identity of replicator(–mutator) dynamics on graphs with quantum strategies in a public goods game," *Dynamic Games and Applications*, mar 2024.

[17] L. E. Blume, "The statistical mechanics of strategic interaction," *Games and Economic Behavior*, vol. 5, no. 3, pp. 387–424, 1993.

[18] A. Correia, L. Leestmaker, H. Stoof, and J. Broere, "Asymmetric games on networks: Towards an Ising-model representation," *Physica A: Statistical Mechanics and its Applications*, vol. 593, p. 126972, 2022.

[19] A. Traulsen, J. M. Pacheco, and M. A. Nowak, "Pairwise comparison and selection temperature in evolutionary game dynamics," *Journal of Theoretical Biology*, vol. 246, no. 3, pp. 522–529, 2007.

[20] V. Pandit, A. Mukhopadhyay, and S. Chakraborty, "Weight of fitness deviation governs strict physical chaos in replicator dynamics," *Chaos: An Interdisciplinary Journal of Nonlinear Science*, vol. 28, p. 033104, 2018.

[21] S. Arigapudi, Y. Heller, and I. Milchtaich, "Instability of defection in the prisoner's dilemma under best experienced payoff dynamics," *Journal of Economic Theory*, vol. 197, p. 105174, 2021.

[22] G. Dal Maso, *An introduction to* Γ*-convergence*, vol. 8 of *Progress in Nonlinear Differential Equations and their Applications*. Birkhäuser Boston, Inc., Boston, MA, 1993.

[23] A. Braides, Γ*-convergence for beginners*, vol. 22 of *Oxford Lecture Series in Mathematics and its Applications*. Oxford University Press, Oxford, 2002.

[24] M. Cicalese and F. Solombrino, "Frustrated ferromagnetic spin chains: a variational approach to chirality transitions," *J. Nonlinear Sci.*, vol. 25, no. 2, pp. 291–313, 2015.

[25] M. Cicalese, M. Forster, and G. Orlando, "Variational analysis of the J_1–J_2–J_3 model: A non-linear lattice version of the Aviles–Giga functional," *Archive for Rational Mechanics and Analysis*, vol. 245, p. 1059–1133, jun 2022.